Machine/Deep Learning Based Adaptive Myoelectric Control

Author

Hassan Ashraf

Registration Number

00000277162

Supervisor

Dr. Asim Waris

DEPARTMENT OF BIOMEDICAL ENGINEERING AND SCIENCES

SCHOOL OF MECHANICAL & MANUFACTURING ENGINEERING

NATIONAL UNIVERSITY OF SCIENCES AND TECHNOLOGY

ISLAMABAD

July 2021

Machine/Deep Learning Based Adaptive Myoelectric Control

Author

Hassan Ashraf

Registration Number

00000277162

A thesis submitted in partial fulfillment of the requirements for the degree of

MS Biomedical Engineering

Thesis Supervisor

Dr. Asim Waris

Thesis Supervisor's Signature: _____

DEPARTMENT OF BIOMEDICAL ENGINEERING AND SCIENCES

SCHOOL OF MECHANICAL & MANUFACTURING ENGINEERING

NATIONAL UNIVERSITY OF SCIENCES AND TECHNOLOGY

ISLAMABAD

JULY 2021

FORM TH-4

National University of Sciences and Technology

MASTER THESIS WORK

We hereby recommend that the dissertation prepared under our supervision by **Hassan Ashraf Registration No. 00000277162** titled "**Machine/Deep Learning Based Adaptive Myoelectric Control"** be accepted in partial fulfillment of the requirements for the award of MS Biomedical Engineering degree with Grade (___)

Examination Committee Members

1. Name: Dr. Asim Waris Signature: _____
2. Name: Dr. Syed Omer Gilani Signature: _____
3. Name: Dr. Amer Sohail Kashif Signature: _____
4. Name: Dr. Umer Ansari Signature: 

_____ _____

Head of Department Date

COUNTERSIGNED

Date: _____ _____

Dean/Principal

Thesis Acceptance Certificate

It is certified that the final copy of MS Thesis written by Hassan Ashraf (Registration No. 00000277162), of Department of Biomedical Engineering and Sciences (SMME) has been vetted by undersigned, found complete in all respects as per NUST statutes / regulations, is free from plagiarism, errors and mistakes and is accepted as a partial fulfilment for award of MS Degree. It is further certified that necessary amendments as pointed out by GEC members of the scholar have also been incorporated in this dissertation.

Signature:_____

Date:_____

Dr. Asim Waris (Supervisor)

Signature HOD:_____

Date:_____

Signature Principal:_____

Date:_____

Declaration

I certify that the following research effort, titled "Machine/Deep Learning Based Adaptive Myoelectric Control," is my original work. The work has not been evaluated by another institution. All additional sources of information have been acknowledged and referenced properly for the material that was used.

Signature of Student

HASSAN ASHRAF

00000277162

Plagiarism Certificate (Turnitin Report)

This thesis has been checked for Plagiarism and the Turnitin plagiarism report endorsed by supervisor is attached.

Signature of Student

HASSAN ASHRAF

00000277162

Signature of Supervisor

Copyright Statement

Acknowledgements

To begin, I would like to thank my supervisor, Dr. Asim Waris, for his constant support of my studies and research, as well as his patience, inspiration, enthusiasm, and enormous wisdom. His suggestions helped me much throughout the research and writing phases of my thesis. For my study, I could not have asked for a more competent advisor and mentor. He has educated me how to do research and present the findings in the most straightforward manner possible. It was a great joy and privilege to work and learn under his guidance. I owe him my gratitude for all he has done for me. I would like to thank him for his friendship and wicked sense of humor as well.

I am also very appreciative of Dr. Syed Omer Gilani's scientific counsel, expertise, intelligent talks, and recommendations. He is my main source for obtaining answers to my scientific inquiries and was crucial in assisting me in completing my thesis. I also want to express my gratitude to Dr. Amer Suhail Kashif, a member of my research committee, for his career guidance and recommendations in general.

I also like to express my gratitude to my colleague, Dr. Imran Khan Niazi, for his assistance and instruction. He is an excellent scientist with excellent communication abilities who has taught me a great deal about research methods. He is an excellent instructor who encouraged and expected me to think critically about the experiments and their findings.

I am very appreciative of my parents' love, prayers, concern, and sacrifices in educating and preparing me for the future. I am grateful to my older brother and mentor Muhammad Naveed for his love, understanding, prayers, and unwavering support in completing this study project.

I would want to express my gratitude to my friends Muhammad Awais Yaqoob and Gulam Fareed for their unwavering support. These two buddies helped me recognize my capacity to do this study. Without them, I would not have endured the worst days of my life. We have all been there for one another and given one other many lessons about life in general.

I would like to express my gratitude to Sameen Mehtab for her assistance throughout my study. Finally, I want to express my gratitude to everyone who has aided me in completing the research work, whether directly or indirectly.

This page is intentionally left blank

Dedicated to my love, Abdul Mannan.

Abstract

Electromyography (EMG) is a method for determining how muscles and the nerve cells that control them operate. To contract and relax the muscles, electrical signals are generated by motor neurons. EMG signals may be utilized to create myoelectric control systems for assistive and rehabilitative devices, whether they are recorded invasively or noninvasively. The performance of the proposed myoelectric control is compromised by a variety of parameters, such as: the channel count, electrode location, noise contained in the EMG data, feature selection, and classifier selection. The goal of this research was to investigate the impact of sophisticated signal processing frameworks on the intrinsic characteristics of EMG signals to enhance the signal to noise ratio of the recorded data. Different EMG filters based on Empirical (EMD) and Variational Mode Decomposition (VMD) were developed and tested to denoise EMG signals. The EMG filter was designed using Clear Iterative Interval Thresholding (CIIT), Iterative Interval Thresholding (IIT), and Interval Thresholding (IT) methods, as well as SOFT, HARD, and SCAD operators. The denoised signals were then transferred to Pattern Recognition algorithms based on Convolutional Neural Networks (CNN) and Linear Discriminant Analysis (LDA). Additionally, disjoint and overlap segmentation methods were used to assess the effectiveness of the optimal windowing configurations. For both surface and intramuscular EMG data, statistical analysis revealed Iterative Interval Thresholding with VMD produces the greatest SNR despite the amount of noise in the signal. Whereas EMD-based filters do not retain the intrinsic properties of intramuscular EMG signals. For both LDA and CNN, statistical analysis revealed that the optimal segment size for disjoint windowing is between 250ms - 300ms. For overlap segmentation, the optimal time range for LDA is 250ms-300ms and for CNN is 275ms-300ms. The settings suggested here may be utilized to create a strong and reliable MEC.

Table of Contents

ABSTRACT **1**

CHAPTER 1 ..... **5**

1.0. INTRODUCTION **5**

1.1 OBJECTIVES 7

CHAPTER 2 ..... **8**

2 BACKGROUND **8**

2.1 FUNDAMENTALS OF EMG SIGNAL 10
2.2 EMG CHARACTERISTICS 14
2.3 MYOELECTRIC CONTROL 15
2.4 PATTERN RECOGNITION BASED CONTROL 17
2.5 MES MEASUREMENT STRATEGIES 17
2.6 SIGNAL DENOISING 19
2.7 SEGMENTATION 19
2.8 FEATURE EXTRACTION 20
2.9 CLASSIFIERS 21

CHAPTER 3 ..... **22**

3 METHODOLOGY AND IMPLEMENTATION **22**

3.1 DATASETS: 22
3.2 SIGNAL DENOISING 23
3.2.1 Empirical Mode Decomposition *23*
3.2.2 Variational Mode Decomposition *24*
3.3 SEGMENTATION 25
3.4 FEATURE EXTRACTION 25
3.5 CLASSIFICATION 26

CHAPTER 4 ..... **27**

4 RESULTS **27**

4.1 EMPIRICAL MODE DECOMPOSITION 27
4.2 VARIATIONAL MODE DECOMPOSITION 28
4.3 SEMG SEGMENTATION 30
4.4 IEMG SEGMENTATION 31

CHAPTER 5 ..... **37**

5 DISCUSSION AND CONCLUSION **37**

5.1 CONCLUSION 39

6 REFERENCES **40**

List of Figures

Electrical signals generated in the muscle fibers.	12
Phase shifted action potentials of a muscle fiber.	13
Superposition of MUAPs to generate EMG signals.	14
Pattern Recognition-based myoelectric control system.	17
Different EMG signals corresponding to different hand motions.	20
Different EMG segmentation techniques.	21
Detailed methodological flow chart of the proposed methodology.	23
Scatter plot of utilized features extracted from EMG signals.	27
EMG signal denoising using different thresholding techniques.	28
EMG signal denoising using different thresholding operators.	29
Classification accuracy corresponding to CNN and LDA with respect to different segment sizes for all the datasets using disjoint segmentation framework.	31
Classification accuracy corresponding to CNN and LDA with respect to different overlap sizes for all the datasets.	32
Classification accuracy corresponding to CNN and LDA with respect to different segment sizes for all the datasets of iEMG signals.	33
Classification accuracy corresponding to CNN and LDA with respect to different overlap sizes for all the datasets of iEMG signals.	34
Classification accuracy for both segmentation techniques for dataset-1 of iEMG signals.	36
Classification accuracy for both segmentation techniques for dataset-2 of iEMG signals.	37

List of Tables

Details of the different EMG datasets used in this study.	23
EMG signal denoising using EMD and VMD based EMG filters.	29
MCAs for dataset-1 across varying window and overlap size.	33
MCAs for dataset-2 across varying window and overlap size.	34

Chapter 1

1.0. Introduction

Upper limb prostheses are used to facilitate the restoring of functionality as well as appearance of the missing limb. The goal is to replicate maximum functionality. The absence of upper limbs hampers routine activities of the affected individual and can cause lags for all those who encounter such individuals. Psychological wellbeing is also at risk of such individuals, along with physical challenges. According to estimates, it has been reported that in 2005 around 664,000 people in the USA had missing limbs and around 900,000 people had smaller limb loss [1]. Moreover, these figures are expected to double by the year 2050 [2]. Global estimations have also reported a marked rise in amputations due to multiple factors such as weapon related violence, accidents, general increase in population, terrorist attacks, natural disasters such as earthquake and tsunamis, and certain diseases like diabetes and vascular problems [3]. It has been reported that 1 in 200 persons in USA faced an amputation related issue from the year 1988 to 1996, and on average, around 130,000 people had amputations in hospital per annum [4].

The results compiled by Yinusa et al. (1989), and Viswanathan et al. (2010) suggest that a significant factor for amputation in developing countries is vascular diseases which account for 25 to 50% of all the cases [5,6]. Another study conducted by Kerstein (1974) reported that vascular diseases caused 75-85% lower limb amputation cases and it was found that 57% of infections were caused due to gangrene [7]. Data from some other studies suggests that 45 to 70% of amputations are done because of diabetes, and this percentage is higher than traumatic causes [8]. However, some researchers conducted in Finland and Denmark suggest that upper limb amputations occur because of trauma as well [9].

In 2005 earthquake, Pakistan reported around 19,700 limb related injuries out of which 78% resulted in amputations [10]. 1115 limb amputations were reported in Sindh, due to traffic accidents, terror attacks, agriculture, medical conditions, gun violence and industrialization [11]. The ratio of affected individuals among males and females was found to be 7 ratio 1, with males being more susceptible than females who have generally low ratio in mechanized work [12].

Prosthetics can be used to perform therapy and replace upper limb amputations by enabling effected individuals to perform daily life activities. The use of prosthetics has been common since 1940s [13]. With the recent advances in technology, the quality of prosthetics has become clinically viable. The frequent use of semiconductors has played major role in developing the technology for clinically applicable prosthetics which has in turn caused a rise in research and development in this field. This technology was introduced in Japan, USA, Canada, Sweden, and USSR in 1960s after the rise of prosthetic related projects [14]. Even with the increasing demand of this technology, there are certain limitations still in way such as embedded actuators, sensors and electronic components which are required to replace original limb and need to adhere to a size limitation. The control of prosthetics needs to replace the original functionality, which is a daunting task.

Upper limb prostheses may be further categorized according to their functioning, namely passive and active prostheses. Passives comprise of the cosmetic and functional prosthesis, and actively make part of the body-powered and externally powered prosthesis. Cosmetic is used to replace the missing limb and does not provide functionality while functional can be used to perform some of the activities as well. Active prosthesis, on other hand, targets the functionality of the original limb and require a lot of energy, which is provided either by the human body or an external power source. In either case, the energy required can be extensive. These active prostheses are further classified into Electric and electromyographic (EMG) controlled.

Myoelectric controlled prosthesis has been reported to be the most feasible as it allows movement in multiple degrees of freedom. Myoelectric controlled prosthetic limbs can be created using both surface and intramuscular EMG signals. We need to design a terminal device which is flexible, allows multiple degrees of freedom for movement and noninvasive, which does not require a big operation. Thresholding of the EMG signal was used to create these limbs, which did not allow for high accuracy and multiple degrees of freedom [15]. Pattern Recognition and Machine Learning based modelling techniques are now being used to address limitation issues, automatically finding patterns in EMG signals, and classifying them [16]. To design such a limb, a four-step method is being employed,

which includes preprocessing, segmentation, feature extraction and classification of EMG signals.

To develop a myoelectric control system for the control of artificial limbs, both intramuscular and surface EMG signals can be utilized. The key characteristics of any such myoelectric control system include intuitive, noninvasive, and robust control providing facility of multiple degrees of freedom (DOF) [17]. Earlier, on-off, finite state machine (FSM), proportional and direct techniques were used for the design of upper limb prostheses [18]. To control the designed prostheses for limited degrees of freedom, conventional control techniques, and the use of amplitude for acquired signal as a threshold was used. Pattern recognition (PR) based schemes provide intuitive and better control with greater number of degrees of freedom for limb prostheses by decoding underlying patterns in EMG signals. Any PR-based MEC can be designed by following data acquisition, preprocessing, feature extraction and classification steps.

1.1 Objectives

The objectives of the study are:

1. To denoise EMG signals by increasing signal to noise (SNR) ratio.
2. To evaluate the effect of thresholding techniques and operators on the performance of Empirical Mode Decomposition based EMG filter.
3. To evaluate the effect of thresholding techniques and operators on the performance of Variational Mode Decomposition based EMG filter.
4. To identify the optimum segmentation technique, segment and overlap size to enhance the performance of myoelectric control system.

Chapter 2

2 Background

The electrical activity generated because of the contraction of the muscles is measured with the help of a technique called the EMG which is the acronym to Electromyography. To produce this electrical activity muscles must be contracted, and the signals must be recorded by using EMG. This electrical signal recorded is called as the electromyogram. Movements performed by the individuals is necessary to generate and record the EMG signals.

The history of EMG started with the study carried out by the H. Piper when he investigated about the electromyography signals with the help of a string type galvanometer in the year 1912 in Germany [19]. Similar studies were made by Erlanger and Gasser with an oscilloscope in the year 1924 [20]. Proebster in the year 1928, revolutionized the study of the EMG by analysing the EMG signals produced in the muscles which lacks the nerves supply(denervation) [21]. He is thus regarded as the pioneer of the domain now called as the clinical EMG. A year later i.e., in 1929, Bronk and Adrian were successful in developing a very potential component that is still in use to record the EMG signals [22]. This tool is known as CNE or concentric needle electrode. As the time passes, the scientists keep on adding the new and modern technologies to better study the EMG signals and EMG. One such step was the utilization of the computer technology. Various kinds of models and simulations were carried out regarding the EMG study with the help of the computers. The years between 1970-1980 was the time during which the field of EMG made considerable progress [23]. As many research articles were published and more and more research findings were documented for the world [24]. A plethora of information about the EMG signal and within the EMG signal was made available. It helped in the study and flourishing of various other fields such as EMG biophysics. Furthermore, to design and develop new approaches and to modify the existing ones, models serves as the primary tool to better understand the EMG as well to train the researchers working in the field of EMG. One of the earliest EMG applications is the extraction of the EMG signals which could serve as the source of input for the power guided prostheses of the upper limb. It was given the name of myoelectric control. The history of myoelectric control is traced

back to 1940s. It made rapid progress during the years between 1960 to 1980 [25]. In the 21st century, the design and development of the diversified powered based prostheses according to the recognition-based controllers by using the EMG pattern is a very notable and well-researched topic in the field of EMG [26].

One of the two types of EMG is the Needle EMG. As the name suggests, this technique uses the needles to record the electrical activation of the muscles. The needle EMG serves the function of detecting the EMG signal from the firing of the motor unit action potential or MUAP at the vicinity near the needle surrounding a very small area. In can thus be useful to gather very concentrated information from the deep as well as the superficial muscles. The second type is called as the surface electromyography. It works by detecting the action potential of the motor units from a large surface area of the muscle. It is helpful in providing the global details regarding the muscular contractions. sEMG is mostly performed to detect the MUAPs of the superficial muscles. At present the surface EMG makes use of the specified electrodes in the form of 2D electrode grids or a linear electrode array [27]. It is thus helpful in implementing the filters particularly the spatial filters as well as allows the in-depth analysis of various parameters of MUAPs individually.

As the muscles are surrounded by the tissues hence, they become the source of interruption between the target muscle groups and electrodes while recording the EMG signals. These tissues have a disadvantage of masking or hiding information. As a result of which there are high chances of the loss of any important information. Thus, it is quite challenging to interpret the signals recorded by sEMG than by the needle EMG. It should also be noted that the sEMG gives the users the ease to record the signals as well as it has a non-invasive characteristic. Hence, it is often preferred by many such as amateur operators and the non-medical lab researchers etc. Because of this reason we can see a wide range of use of sEMG in variety of applications such as in the assessment of fatigue, biofeedback system and in the analysis of movement. This incorporation thus has become the cause of chaos due to lack of standard guidelines for its operation because of which the EMG signals data is compromised. One proof is that all those research papers which were published during the past 20 years have contradicting results and facts which is becoming a source of confusion for the other researchers at present [28]. It can thus be said that the widespread utilization

of surface electromyography in various applications has made it kind of unreliable due to the very reasons discussed above. In short, the modern-day EMG has now become very easy to take recordings because it is very easy for the user or any other researchers working in this field to mount the pair of electrodes on the targeted muscles followed by the signal acquisition and signal analysis. From which conclusions can be extracted based on the findings particularly about the EMG patterns, the modalities, its timings as well as the rate at which the muscle is activated.

Present day EMG involves both the needle EMG as well as the surface EMG techniques. Both are the consolidated and interdependent instruments for the EMG signal processing. They both holds a crucial position for the investigations involving the physiological parameters. The needle EMG has a widespread use in the field of diagnosis. On the other hand, the fields such as ergonomics, analysis of motions, sport medicine, occupational medicine, prosthetic control devices and biofeedback mostly uses the sEMG for the major reason that it is harmless and allows the painless and frequent examination of the functions of neuromuscular system. It has also been noted that the uses and the applications of sEMG are mostly ignored and are not covered in the academia [29]. Hence, the major focus is on the use of non-invasive sEMG in the various applications.

2.1 Fundamentals of EMG signal

The study of EMG as stated earlier is the record of the electrical activity generated a result of the muscular fibres contractions. Because of the relationship between the EMG and torque, the EMG thus serves as an appealing to carry out the measurement of the tension in the muscles which is a requirement for the number of physical examinations in a person [30]. But the complex nature of the origin of this signal of EMG is hampering the development of an elaborated description to explain this relationship quantitatively. Hence to comprehend the difficulty level that is a barrier between the EMG and torque, it is thus vital to have an understanding of the origin and character of the EMG signal.

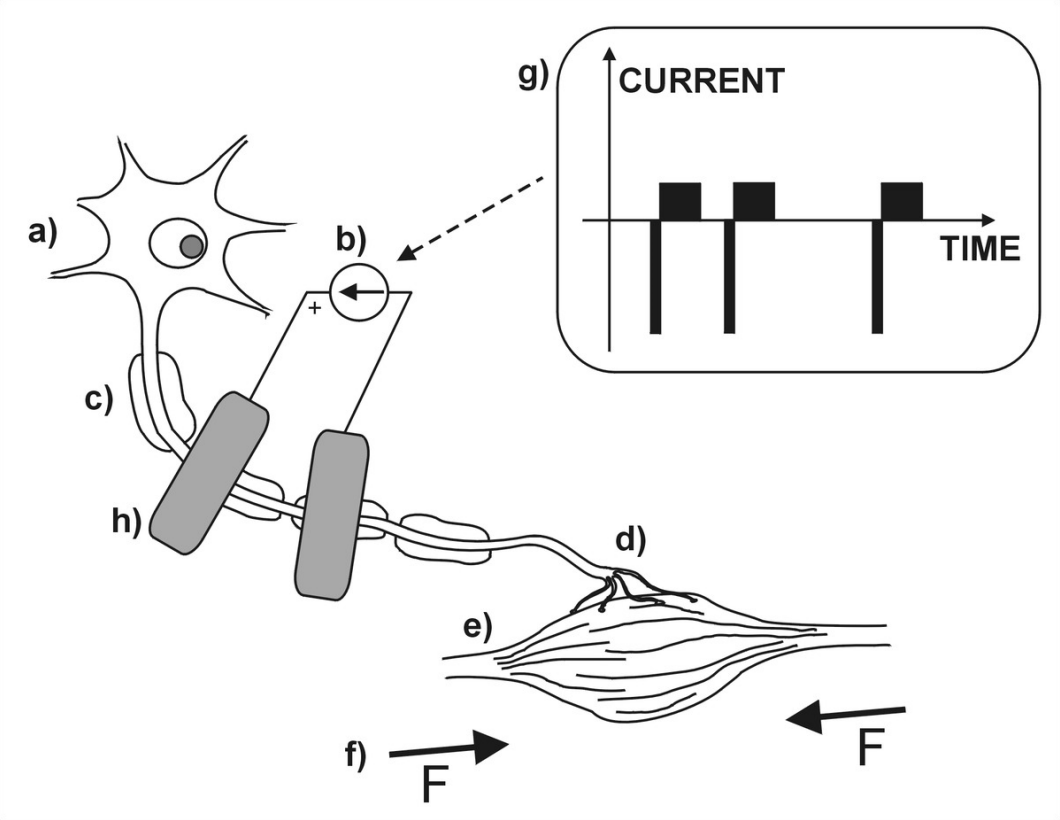

Figure 1. Electrical signals generated in the muscle fibres.

The neuromuscular component is responsible of the human body's voluntary movements, i.e., contractions and relaxations of different body parts. A neuron generates a very tiny potential difference on the membrane of the muscle cell to initiate contraction. This results in elevation of the motor neurons and the subsequent appearance of a depolarization pattern. The waveform generated is then sent to the neuron's terminal end, where it is termed to as the Postsynaptic Neuron, or AP for shorthand. The electrical activity produced by the muscle fibre is shown in Figure 1.

By transmitting nerve branches to muscular tissue in clusters called motor units, a single motor neuron stimulates it. Muscle fibres, which range in size from a few nerve fibres in tiny muscles like the hand and fingers to hundreds of motor neurons in large muscles like skeletal muscle, are the basic unit of contraction. Because each motor unit contains numerous muscle fibres that are connected to the motor neuron in various locations, the electrical signal generated by that unit is the sum of the membrane potentials of all the

muscle fibres in that unit, and that might be transition period relative to the other motor neurons in that unit [31].

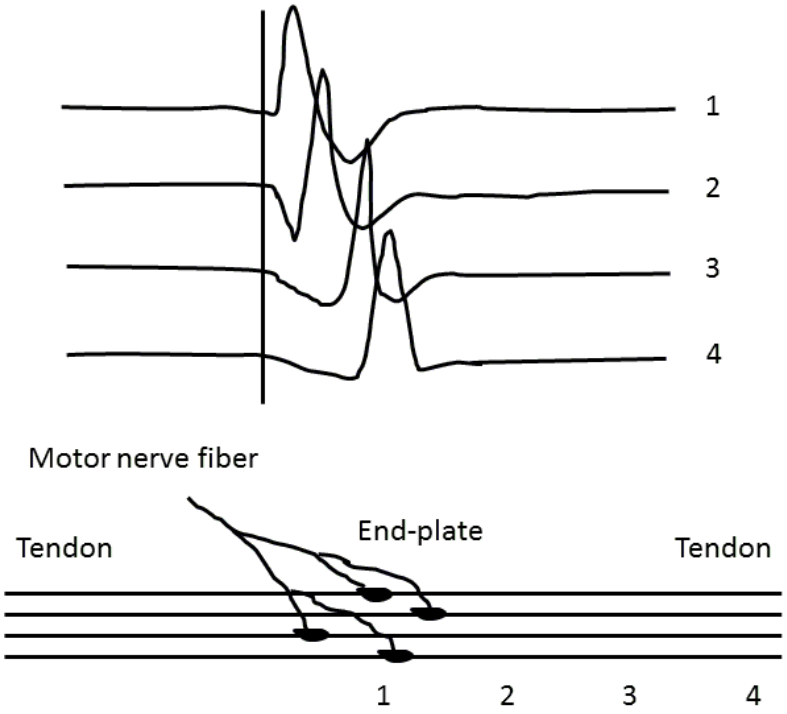

Figure 2. Phase shifted action potentials of a muscle fibre.

Figure 2 demonstrates this idea further. The Motor Unit Action Potential is the electrostatic interaction produced when all neurons in a muscle fiber contract simultaneously following excitation (MUAP) (MUAP). This MUAP may be captured using sensors installed on the scalp above the tissue. Additionally, a single action potential rarely activates a muscle. To maintain a stretch for a prolonged period of time, the nerve cells should be triggered periodically. That recurrent stimulation generates a series of MUAPs, which may have been regarded to as a pulse in traditional signal processing terminology [32]. These grouping of MUAPs is termed to as a Motor Unit Action Potential Train (MUAPT) (MUAPT). Emg is characterized as the convergence of numerous asynchronously firing MUAPTs when monitored with a surface electrode. The idea that surfaces EMG is generated by the superposition of visual evoked potentials is corroborated by Figure 3 [33]. The surface electromyography signal is usually between 5 and 10 mV in magnitude, with the bulk of the signal data contained between 15 and 400 Hz [34]. As a result, the EMG volume accounts for a large proportion of the data transmission that can be represented by

a Gaussian stochastic function. The intensity of a Received signals is specified as the time-varying confidence interval of the signal and is a measure for the muscle strength exercise intensity.

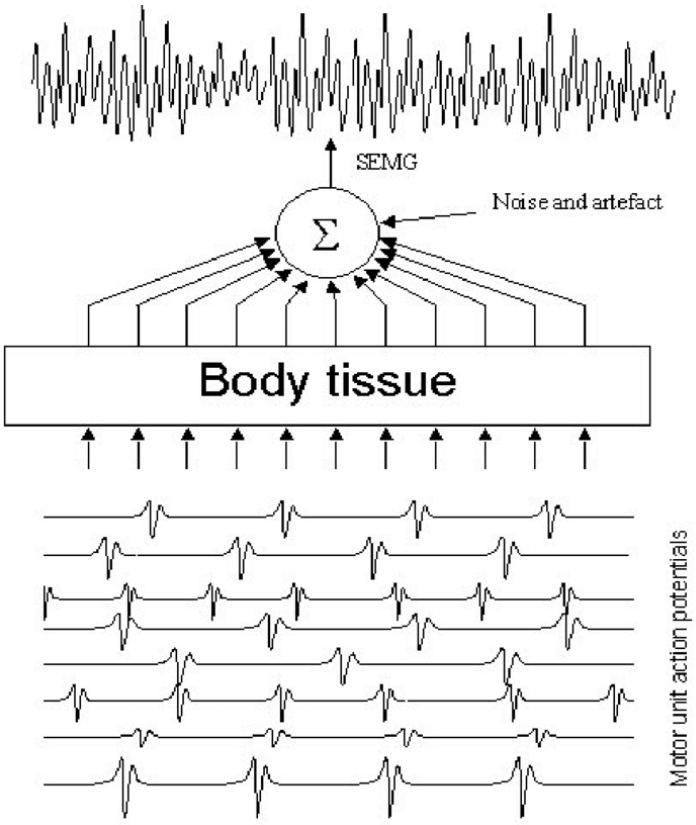

Figure 3. Superposition of MUAPs to generate EMG signals.

Antiagonist-antagonist muscles are found in a variety of human joints. The activation of such a human joint often involves a large number of muscles. The muscles that control the movement of the arm, wrist, and hand are discussed next. The pectoral muscle is responsible for arm retraction. While there are additional muscles in the mammalian forearm, it is primarily controlled by two adjustable heights: the forearm and wrists. As a result, the forearm and a portion of the wrists are fundamental premise muscles [35]. The elbow angle and impedance may be varied at random by changing the amount of force exerted by these muscles. The triceps flexor digitorum muscles contract, causing the elbow to flex. The elbow is extended when the triceps brachii is contracted. The forearm contains the bulk of the tendons that lift the wrist and palm. The abductor supraspinatus radialis is

in charge of wrist extension and abduction. The wrist is flexed and adducted by the flexor digitorum ulnaris.

2.2 EMG Characteristics

In the signal analysis, when the electrical contractions of the muscles are recorded with the help of needle electromyography it can be either semi-periodic or pseudorandom [36]. To investigate the semi-parodic signals, we make use of the various determining variable that are used to describe the isolated MUAPs as well as any other waves [37]. It means that it is possible to observe shape, time as well as the amplitude of the signals. While the pseudorandom signal can be calculated by applying various models from the statistics.

As far as the frequency of the signal is concerned it is affected by various factors. First, while recording the electrical activity of the muscles, the signal is also affected with the intramuscular electrical activity of the tissues which affects the volume conduction [38]. In this scenario, all the high frequency contents present in the signals undergo attenuation more as compared to the low frequency contents present in the signal corresponding to the increase in the distance of action potential generators at the site of the electrode surface. It has been observed that small surface and high input resistance or impedance of the active electrodes tend to show much finer high response in terms of frequency and vice versa [39]. When the electrical activity is recorded by the sEMG, the frequency components of such a signal are always below 500 Hz [40]. While for the single -fiber EMG electrode the maximum frequency is 10kHz and it is 2kHz for the CNE [41]. This knowledge of frequency content is beneficial in physiological studies. The analysis of frequency is mainly used to study the muscular fatigue with the help of sEMG mostly. However, we can see similar results by using the needle EMG. Moreover, for the needle EMG, the study of chronic neurogenic states showed deviation towards the lower frequencies and myopathies showed a deviation towards the high frequency components [42].

Next parameter is the amplitude. The amplitude of any EMG signal is dependent of the similar factors as that of the frequency. Most important of them are Electrode size, distance between the electrodes and the AP generator [43]. When a single-fibre EMG electrode is used to measure the amplitude of a single MUAP it comes out to be between 0.3mV and 10 mV [44]. The strength of the fibres which are acting as the powerful electrical generators

do not have much effect in this case. Thus, we can state that the use of Aps amplitude for a single-muscle fibre cannot be used for the diagnostic criteria for the single fibre EMG. The use of concentric needle electrode guarantees the more promising results to record the amplitude of MUAP. Because in this case the distance changes are very small. Lastly, the dependence on the distance for the macro-EMG is much lesser compared to the former two thus it is safe to say that the amplitude of the macro- MUAP shows the action potential's generator strength [45].

2.3 Myoelectric Control

To develop the power-based prostheses the surface myoelectric signals obtained from the surface EMG serves as a significant and efficient input system. In the technical terms, this application of control is known the myoelectric control. It has now become a famous domain due to its massive use by the people born with upper limbs congenital amputation or having amputated limbs due to any injury or an accident etc. This system is designed in such a way so that it can voluntarily control the selection as well as the regulation of the multi-dimensional prosthesis [46]. The concept is based on the similar voluntarily controlling ability of the various parameter of the myoelectrical signals obtained from the muscular groups or a single muscle. A schematic representation of the necessary components to design such a control system is shown in Figure 4. In this diagram the motor control system is replaced with the feedforward pathway which is denoted a myoelectrical channel.

Control signal's source for myoelectric controllers is viable residual muscle remaining following amputation or available muscle in the case of a congenital limb deficiency. Given a large superficial muscle and a surface closely spaced bipolar electrode pair, it is possible to acquire myoelectric signal from this muscle alone and achieve a single muscle control channel [47]. Indeed, with a fine wire intramuscular bipolar electrode it is possible to isolate a small muscle segment and use the motor unit action potential trains as control signal sources. Clinically, however, this latter signal source is not practical due to the invasive transcutaneous nature of the electrode [48]. For surface electrodes the limitations of the single muscle source include the requirement for a superficial muscle, the small interelectrode spacing, and in the case of the congenital amputee the uncertainty of muscle position.

In contrast to the single muscle myoelectric channel referred to above, a widely spaced electrode pair appropriately placed on the limb will acquire signal from a muscle group. Such a multi-muscle control signal source is the temporal and spatial sum of the electrical activity of the muscles of the group. The practical limitations of achieving a single muscle source mean that the multi-muscle source is the more common control source. It is simply easier to put a widely spaced electrode pair on the limb and use all available signals, rather than searching for critical positions on individual muscles. It is also the case, from a control information point of view, that the temporal and spatial sum of the signals from muscles of a group has certain advantages over a single muscle [49]. This follows from the observation that the contribution made by each muscle of the group to the sum is a function of the intended limb action. Thus, the contribution pattern can be voluntarily controlled, and the pattern used for control purposes.

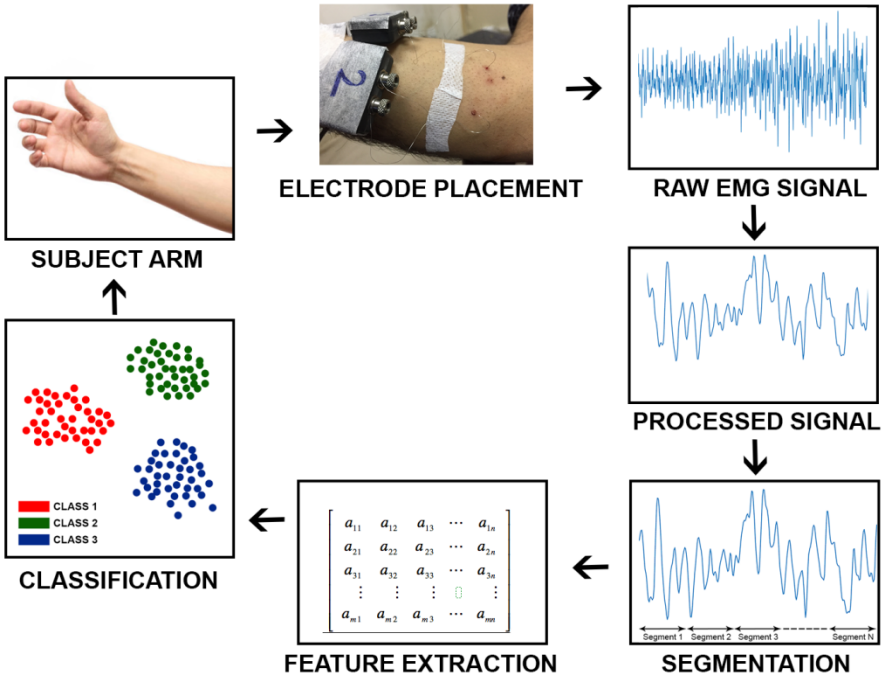

Figure 4. Pattern Recognition-based myoelectric control system.

Following are the major elements needed to design a myoelectric channel; single or a group of muscle, an electrode, and a conduction device to carry out the volume conduction in between the electrode and the pair of muscles [50]. In remaining section, the control information potential of a single channel and a multichannel will be presented.

2.4 Pattern Recognition Based Control

To level up the order of devices to make the control of the myoelectric signal more efficient, there is a need to design a rather more modernized strategy that could be able to differentiate between the variable motion states of the targeted muscle. A pattern recognition-based myoelectric control system is depicted in figure 4. It could be accomplished by the following two approaches [51].

1.1. Firstly, the system is desirable to be able to extract additional information regarding the muscular activity in its active state. To achieve this, any of the two or both ways could be employed.

- To fetch the exclusive information about the targeted muscular groups the system must be able to use various MES channels.
- Other is the development of the sets of features that must be able to extract the maximum information from the input signals and able to differentiate between the distinct categories of the motions.

1.2. Lastly, a classifier must be constructed that is capable enough to make the most out of the extracted information. This classifier plays an important role for utilizing and assimilating this input information and then determine its respective origin class of this information.

2.5 MES Measurement Strategies

When using the surface myoelectric signal, the primary concern regarding the placement of recording electrodes is to capture as much novel information about the muscle activity as possible. To accomplish this, when placing electrodes on the upper limb, one is faced with two possibilities:

1.1. A single bipolar channel, with the bipolar electrodes spaced widely apart. This technique, used by Hudgins [52], involves placing one electrode on the biceps and one on the triceps. This approach captures the activity of a large volume of muscle, all superimposed into a single gross myoelectric channel. The drawback of this approach is that there is no spatial discrimination in the activity of different muscles, and novel information from different muscles may exhibit destructive interference.

1.2. Multiple bipolar channels, with closely spaced electrode pairs. Because the pickup region under closely space pairs is more local, multiple channels are needed to capture the activity of different muscle groups. The advantages address the drawbacks of the single channel; spatial discrimination is now possible, and no destructive cancellation occurs.

It has been shown in several studies that multiple MES, channels provide much better discrimination among control states than do single channels [53,54]. The nature of the myoelectric signal in specific has the potential to impact and guide the control signal in terms of its competencies. It should be noted that the research protocols designed by the previous scientists carried out contractive recordings of the MES or myoelectric signals in a constant or in other words steady state environment [55]. The output is a randomly generated signal most of the time when its properties were analysed statistically as discussed earlier. The specified patterns of neuronal firing for carrying out the contractions as well as the need to actively modify the recruited motor units leaves a very minimal temporal or the time-dependent structure for the steady-state of myoelectric signals.

The effects of these myoelectric signals in concurrent to the active contraction initiation was well researched by the Hudgins and companions. The findings demonstrated a significant presence of the structure viewed in the waveform having the transitory nature. The results can be visualized in the figure 5. The figure represented the local behavioural patterns in conjugate to the pronation as well as the supination orientations of the forearms. Moreover, the elbow flexion and extension can also be seen in the figure. The data was collected from the muscular activity of the biceps and triceps in the arm. These muscle groups were mounted with the single pair of the bipolar electrodes for the recordings. The focus was to cover a major part of these musculoskeletal regions for the better efficiency.

When these waves were analysed in their time-domain it showed prominent contrasts in the patterns under considerations. Meanwhile, the analysis of the groups of patterns which were obtained at a particular rate of contractions presented that their corresponding structures are enough to demonstrate the visual distinctive differences for varying contraction rates. Many other researchers also described the presence of this visible layout [56]. It showed a well-ordered assimilation of the neuronal units of brain called the motor

units. This may result from a “motter plan” located at CNS, absence of sensory feedback paths within such a rapid burst of activity, or a combination of both.

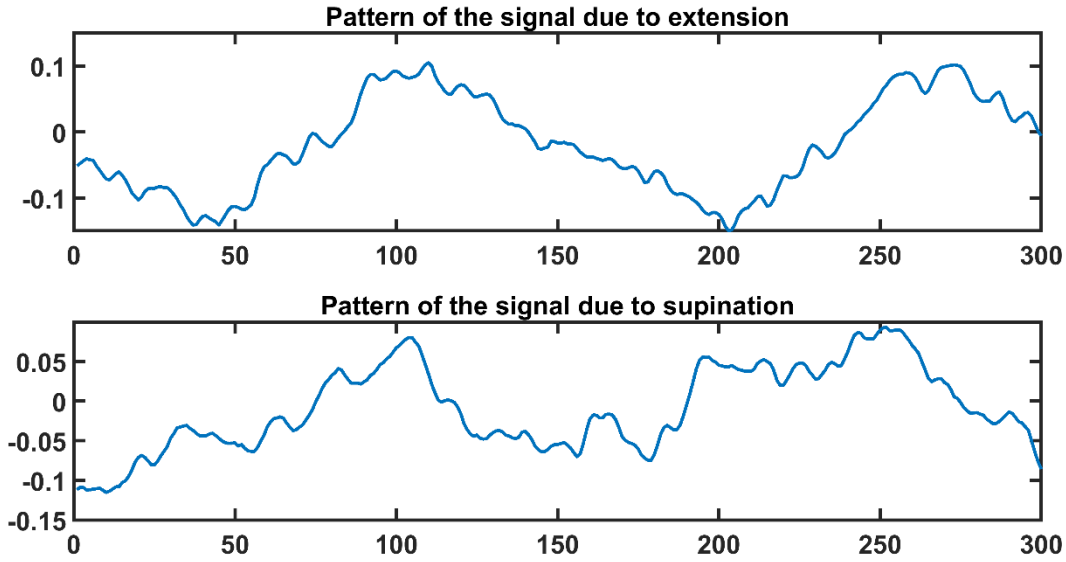

Figure 5. Different EMG signals corresponding to different hand motions.

The presence of determinism in the transient MES accompanying the onset of contraction suggests that these data should provide a powerful means of discriminating MES patterns corresponding to different movement types. This has been demonstrated by Hudgins et al. in a prosthetic control system, which will be described below, and by Farry et al., with application to teleoperation of a robotic hand [57,58].

2.6 Signal Denoising

For any application or for an appropriate interpretation of an EMG signals for investigating muscle activity, the prerequisite is the acquisition of clean EMG signal. Like other physiological measurements, EMG recordings are contaminated with different type of noises i.e., Baseline Wandering (BW) or motion artifacts, White Gaussian Noise (WGN) and Power Line Interference (PLI). Therefore, the identification of actual and real EMG signal remains difficult and challenging [59].

2.7 Segmentation

Every peak gives the data about the original signal for various biological signals, such as ECG. As a result, these signals are divided into segments based on their shape. Individual

peak does not give enough details of PR-based MEC in the case of EMG signals. EMG signals are also studied throughout segments of varied time since they are non-stationary, meaning their statistical features fluctuate with time. A single signal segment may function as a query for data in a particular time slot, assisting in the prediction of the signal stream's overall features and attributes. A lengthier portion contains more information about the original signal. Increased segment length, on the other hand, causes a greater hardware complexity for actual PR-based MEC [60]. There is an exchange between processing speed and section description correctness as a consequence of this exchange. A small chunk is more vulnerable to volatility and bias in feature extraction, as well as noise, due to its shorter length.

A segment with a length of less than 200ms is insufficient to reflect the original signal [61]. A segment should be larger than 200ms for better reproduction of the original signal in real-time MEC and offline. For seamless and real-time operation, a real-time signal restricts with 300ms limits so, the segment size should be less than 300ms [62]. There are two distinct kinds of segmentation, as shown in Figure 6. A disjoint segment's length is governed only by its span, while an overlapped section's length is dictated by both its duration and the threshold value (adjustment). The time variance sequential segments, known as the leap or gap, will be smaller than the lengths but greater than the MEC processing time.

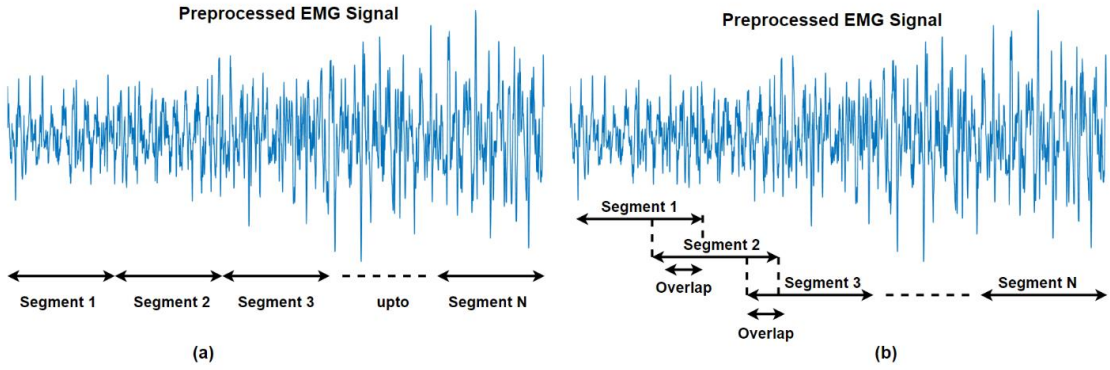

Figure 6. Different EMG segmentation techniques.

2.8 Feature Extraction

The most intuitive, and most widely used, feature that describes the MES has been the index of gross activity, which be the variance, mean absolute value, or some other similar

measure. Multivariate features sets have been presented and effectively employed with the goal of delivering additional information about the MES in each channel [63]. At first, limited by the available computational power of the day, the features were based on time domain statistics, such as variance, zero crossings, and the "length" of the waveform locus. With increasing computational resources came systems based on autocorrelation time series models, spectral measurements, and coefficients. Using the short-time high order spectrum analysis, wavelet and wavelet packet transforms, Fourier transform, current approaches attempt to utilize the temporal structure of MES patterns [64].

2.9 Classifiers

The practical approaches for pattern classification that exist can be divided into three categories. Historically, the statistical and syntactic approaches have been the two most common ways [65]. The learning (or neural) technique is the third and most recently established type of pattern classification. Perceptrons and adaptive linear components are the origins of learning algorithms, which have evolved into the broad field of artificial neural networks. In terms of the use of classifiers in MES control systems, statistical classifiers were used almost exclusively until about the mid-1980s, at which point the first applications of artificial neural networks began to appear [66]. A variety of artificial neural networks architecture and learning algorithms have been investigated in the context of MES pattern recognition, including simple feed forward multilayer perceptrons, dynamic networks, and self-organizing feature maps. Recent investigations have seen the application of genetic algorithms and fuzzy logic classifiers [67]. If a consensus can be drawn from these investigations, it is that although powerful classifiers may marginally improve the classification of the MES, it is the feature set that is crucial to overall performance.

Chapter 3

3 Methodology and Implementation

3.1 Datasets:

Surface EMG data from 30 individuals was divided into three datasets for the research. The National University of Science and Technology's local supervisory commission approved all data collection (approval number: ref# NUST/SMME-BMES/REM/00321/30012021). All participants completed a written permission form before to the experimental procedure. Ten healthy individuals (5 men and 5 females, ages 21 to 32) participated in dataset-1. These individuals had no prior history of musculoskeletal problems. Thalamic Lab developed the MYO wristband EMG sensor, which can be used to capture surface EMG data and is commercially accessible [68]. The MYB encompassed the extensor carpi ulnaris, extensor digitorum, palmary longus digitorum superficialis, extensor carpi radialis, and flexor Capri radialis muscles, and it was tied to the subjects' dominant wrist. The tests were conducted on the BioPatRec EMG platform, which is open to the public, and each participant was asked to perform at least eleven agile hand movements [69].

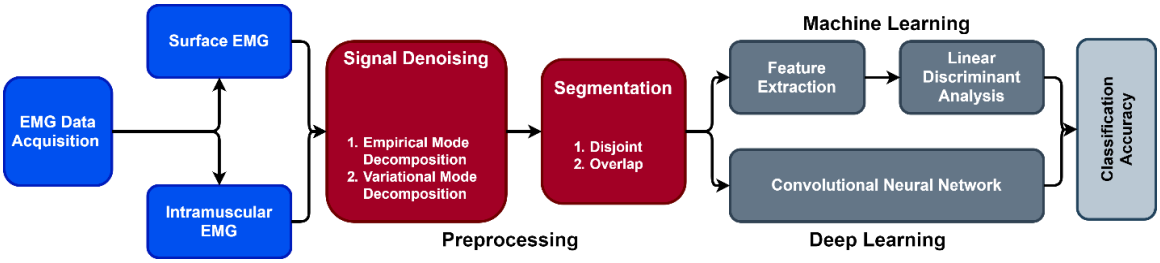

Figure 7. Detailed methodological flow chart of the proposed methodology.

Individuals were displayed each activity before recording it using the BioPatRec interface. Supination, Open hand, Close hand, extend hand, Flex hand, Agree, Pointer, Fine Grip, Side Grip, and no-motion condition were employed in the experimental method. The data for each participant were gathered in a single session and put into a database. Each exercise lasted ten seconds, with six seconds devoted to contraction and four seconds to relaxation.

Dataset-2 was acquired from [70] and utilized. It has a sample frequency of 2000Hz. There were a total of eight active hand movements. The same hand movements were recorded in this dataset. Figure 7 illustrates the full methodological flow chart.

Dataset-3 was also captured ahead of time and utilized in [71]. A widely viable myoelectric generator was used to acquire it. Ten people took part in the study, each having 11 active hand motions. The same motions were also captured in this dataset. The EMG signals were also routed through an analogue passband with trimmed wavelengths of 10-500Hz while being captured. More information about the three datasets used in this research can be found in Table 1.

Table 1. Details of the different EMG datasets used in this study.

	Dataset-I	**Dataset-II**	**Dataset-III**
Subjects	12	11	7
Movements	10	10	10
Channels	6	6	5
Sampling Frequency	2000	200	800
Resolution	16	6	10
Cycles	10	10	10

3.2 Signal Denoising

3.2.1 Empirical Mode Decomposition

An adaptive method introduced for analysis of non-linear and non-stationary signals is Empirical Mode Decomposition (EMD). It is applicable for data driven local separation in slow and fast oscillations. Theoretically, EMD is like Fast Fourier Transform (FFT), however, in FFT the signal is changed to frequency spectrum from time spectrum. The difference between FFT and EMD is that in EMD signal remains in time domain and it is not assumed to be periodic and can be termed into its Intrinsic Mode function (IMF). The EMD can be used on different datasets and no assumptions for the data need to be made, whereas an IMF which is a mono-component function and obeys the following mentioned two criteria [71]:

- Zero crossings and extrema needs to be same or have a difference of one.
- At any given point, local minima envelop and mean of local maxima envelop is zero.

The above stated criteria restricts an IMF to be composed off only a single oscillation per cycle and each cycle is defined based on the number of zero crossings. Riding waves are not allowed, because they can cause negative frequencies which is a major issue in instantaneous frequencies-based application [72]. EMD works on basis of instantaneous frequency which can be defined as per application. An iterative mathematical process called Sifting is used in EMD to decompose any given signal into its IMF components [73]. Local mean is subtracted from input signal in the process of sifting. Envelopes are used to create local means and are therefore subsequently used for finding all the components of IMF. The last component found has lowest frequencies and is used to represent the overall trend, conversely, the first IMF contains the highest frequency components.

3.2.2 Variational Mode Decomposition

The Wiener filter is extended to several adaptive bands using the variational mode decomposition (VMD) approach. The VMD technique converts the model estimate problem into a variational problem and continuously updates the model and its center frequency [74]. Finally, the model is translated to the time domain using the inverse Fourier transformation. The model may be used to generate a series of models and their corresponding center frequencies, which can then be used to recreate the input signal. Furthermore, each mode is smooth after demodulation.

It is a variational model in which the relevant bands are defined adaptively, and the appropriate modes are estimated concurrently, so ensuring that errors are appropriately balanced between them. To find an ensemble of modes that resume the input signal optimally, either in a least-square sense or exactly as we desire, we look for and ensemble of modes that are band-limited about a center frequency that is calculated on-line [75]. When there is noise in the input signal, our variational approach is particularly effective in dealing with this issue. Indeed, the close relationships between our approach and the Wiener filter suggest that our strategy is somewhat ideal in terms of dealing with noise. After complex harmonic mixing has been used to shift the Hilbert-complemented, analytic signal down into baseband, different model determines the bandwidth of the modes as the -norm parameter [76]. In the end, the optimization scheme is quick and easy: Every mode is upgraded in Fourier domain, and the narrow-band wiener filter correlate with mode's center-frequency with the given current on the applied on the signal, all mode estimated

residuals and because of this calculation, the center frequency of the mode's power spectrum is recalculated as the mode's center-of-gravity frequency is recalculated as the mode's center frequency of the mode's power spectrum.

3.3 Segmentation

Because larger segments produce better results in PR-based MEC, colloidal segmentation is applicable for the employ segment lengths more than 200ms for the current real-time constraints and ensures smooth MEC operation. The recorded information used for the segmentation process in both windowing strategies to see whether windowing methodology, step/overlap size and window size provided accurate result of EMG signals. All techniques used 19 distinct window widths, with window lengths ranging from 25 - 500ms in increments of 5ms. Comparably, nine alternative leap sizes were utilized for overlap windowing, ranging from 19% to 80% of the initial duration with a 10% improvement in overlap size width.

3.4 Feature extraction

Following vectorization, the next step was to retrieve useful characteristics within each frame that could be used to distinguish between different types of windows. EMG signals have a number of statistical characteristics that enable for accurate reconstruction of the actual input Certain slope coefficients (features) could perhaps be able to categories objects and may be assessed in the frequency or temporal domains. The amplitude of the signal is used to evaluate time domain properties. In the spectral space however, the power spectral density is used to approximate the same (PSD). A set of EMG data has the best possible class separation, resilience, and computing cost. Waveform length, cardinality, average exact value, neutral point, and slope sign change were all investigated in this study. Figure 3 depicts a scatter plot of all extracted attributes for one participant from dataset-1 for three hand motions for which all recovered attributes were collected.

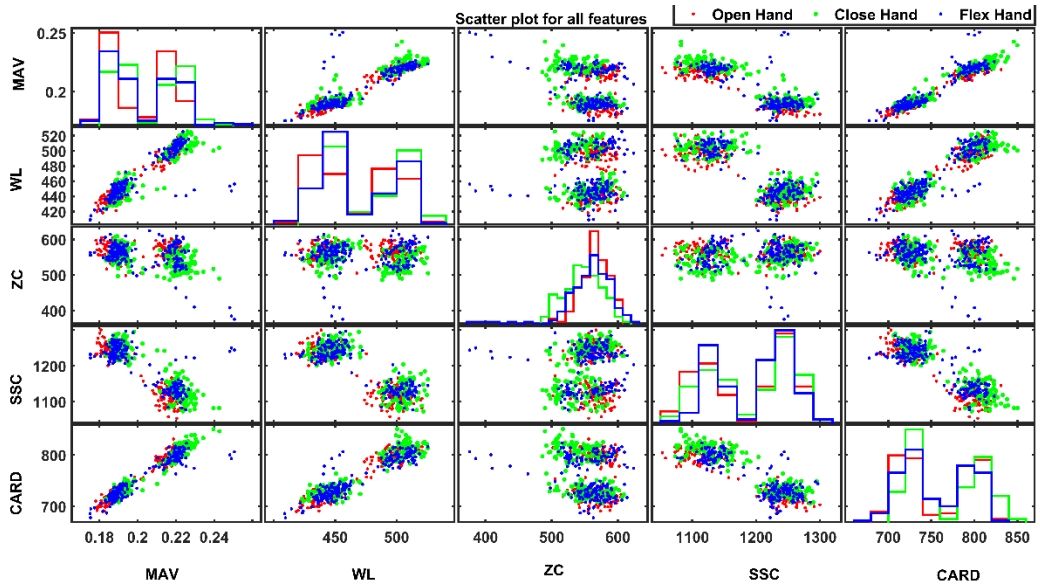

Figure 8. Scatter plot of utilized features extracted from EMG signals.

3.5 Classification

The final data set was then fed into LDA and CNN, which were utilized to categorize iEMG signals. The classification accuracy (CA) has been assessed in order to establish the classifier's overall performance. To every database, windowing technique, and frame size each participant's classifier was trained, validated, and assessed separately. The data from each individual was meant to prepare the network 70% of the time, verify the model 20% of the time, and test the model 10% of the time. EMG data from the publicly available MATLAB toolbox "BioPatRec" [77] was analyzed using LDA. The CA of each subject's test results was calculated and kept track of. Using ANOVA, the effect of sliding window and vectorization technique on iEMG signal prediction accuracy was investigated and shown to be significant. For the purposes of evaluating the statistical tests, likelihood values less than 5percent were considered significant. Several variables were compared using Tuckey's honest post-hoc test.

Chapter 4

4 Results

4.1 Empirical Mode Decomposition

To illustrate and assess the effectiveness of EMD for filtering EMG data, EMG signals were denoised using IT, IIT, and CIIT thresholding methods. Along with the aforementioned thresholding method, three commonly used thresholding operators SOFT, HARD, and SCAD were examined. The Signals were obtained from a pre-recorded database; a total of 15 EMG signals were obtained from five healthy individuals. Due to the nonstationary and stochastic character of EMG data, denoising was conducted on EMG signals with varying amounts of noise. The effectiveness was quantified with respect to signal-to-noise ratio (SNR) pre and post signal preprocessing.

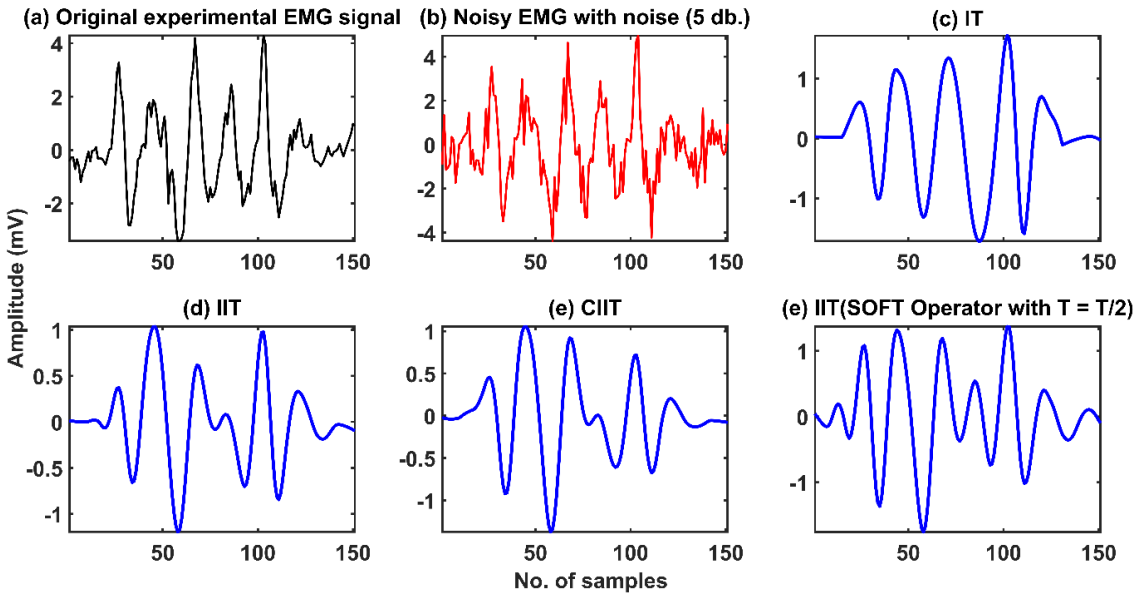

Figure 9. EMG signal denoising using different thresholding techniques.

To determine the optimal thresholding method for noise reduction from EMG signals, simulated noise with SNR values of 0db, 5db, 10db, and 15db was injected into the observed data initially. The noisy samples were then denoised utilizing thresholding methods from IT, IIT, and CIIT. The results indicate that all three thresholding methods examined substantially reduce noise in signals, regardless of their noise level. Table 2 illustrates the performance of the thresholding methods and thresholding operators. As

demonstrated in table 2, the IIT thresholding approach produces a greater SNR than the IT and CIIT thresholding techniques at each noise level and with each thresholding operator, regardless of the kind of thresholding operator.

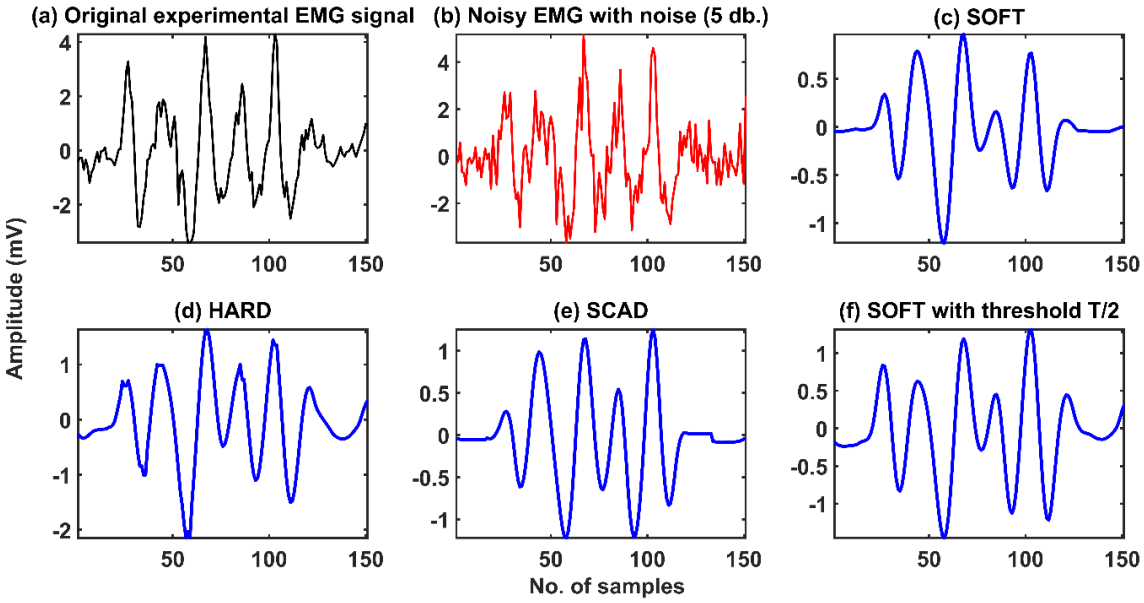

Figure 10. EMG signal denoising using different thresholding operators.

As shown in table 2, the HARD thresholding operator provides the best denoising outcomes for EMG signals at all denoising levels and using all thresholding techniques in terms of SNR. Statistical research revealed that the HARD thresholding operator beats all other thresholding operators tested at the 0dB. noise level (P-values 0.05). The HARD operator produced the highest mean SNR of 7.75 dB, while the SOFT and SCAD operators acquired mean SNR values of 7.35 dB and 4.04 dB, respectively. Similarly, at 5 dB, a quantitatively significant difference in SNR values was found between the HARD operator and both the SOFT and SCAD operators (P-values 0.05). The HARD operator produced the highest mean SNR of 11.65 dB, while the SOFT and SCAD operators generated mean SNR values of 10.39 dB and 7.49 dB, respectively.

4.2 Variational Mode Decomposition

To assess the new method's denoising impact, it is compared to the conventional EMD and VMD techniques. Additionally, the Signal-to-Noise Ratio (SNR) and Root Mean Square

Error (RMSE) are computed between the original signal and the denoising sEMG signal without noise interference.

Table 2. EMG signal denoising using EMD and VMD based EMG filters.

Surface EMG						
Before	**EMD_IT _SOFT**	**VMD_IT _SOFT**	**EMD_IIT _SOFT**	**VMD_IIT _SOFT**	**VMD_IIT _HARD**	**VMD_IIT _SCAD**
0	3.2124	3.1914	3.4367	3.8504	1.7209	2.7965
5	5.9197	8.4684	6.1618	9.1861	6.8872	8.0797
10	8.9177	13.9920	9.1820	14.6343	12.1536	13.5778
15	10.9532	19.3796	11.3534	19.8387	17.3852	19.0084
Intramuscular EMG						
Before	**EMD_IT _SOFT**	**VMD_IT _SOFT**	**EMD_IIT _SOFT**	**VMD_IIT _SOFT**	**VMD_IIT _HARD**	**VMD_IIT _SCAD**
0	1.4578	3.1088	1.5022	3.6711	1.6842	2.7286
5	2.1905	8.2633	2.2406	8.6978	6.9245	7.9814
10	2.5668	12.6907	2.6683	12.6627	11.6353	12.3554
15	2.6071	15.6944	2.8577	15.0898	15.2821	15.2803

As shown in the table, VMD-based EMG filters beat EMD-based filters in terms of SNR for both sEMG and iEMG signals. Additionally, it should be emphasized that SOFT thresholding operator outperforms all other thresholding operators in terms of performance. IIT produced the greatest SNR values for sEMG signals, regardless of the noise contained in the EMG signals. However, for iEMG signals, IIT results in the greatest

SNR values for noise levels of 0 and 5dB, whereas IT results in the maximum SNR values for noise levels of 10 and 15dB.

4.3 sEMG Segmentation

In the case of LDA with disjunct separation, the mean classification score improves substantially when segment length is extended from 50ms to 225ms (P-value = 0.05). From 50ms to 250ms, the MCAs of all datasets rose by 20.18 percent, 6.25 percent, and 9.78 percent, respectively. There has been no substantial difference in MCA fragment sizes between 225ms and 450ms (P=0.44) after 225ms. As only a 2.48 percent, 0.73 percent, and 1.09 percent rise in the MCAs of all datasets, respectively, has been observed. Similarly, when overlap segmentation is compared to LDA, a significant rise of 17.64 percent, 6.73 percent, and 9.69 percent in the MCA values of all datasets from 50ms to 250ms was observed (P-value0.05). Increase in segment length from 250ms to 450ms results in increases of 5.02 percent, 1.1 percent, and 0.93 percent, respectively, in the MCAs of all datasets (P-value=0.07).

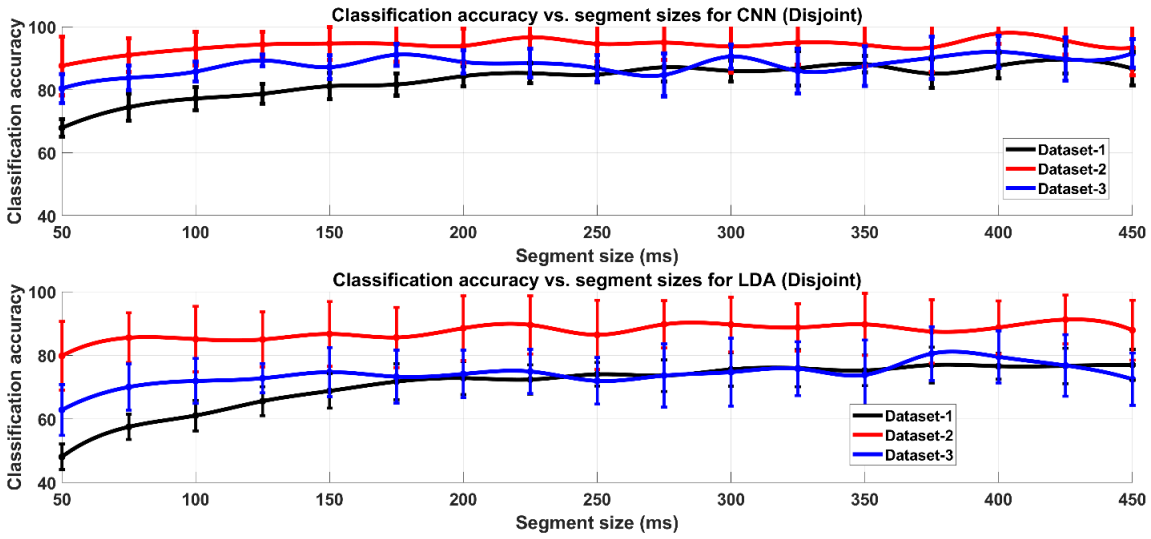

Figure 11. Classification accuracy corresponding to CNN and LDA with respect to different segment sizes for all the datasets using disjoint segmentation framework.

When segment width was raised from 50 to 250 milliseconds using CNN and discontinuous segmentation, MCA rose by 27.16 percent, 9.87 percent, and 11.43 percent for all datasets, respectively (P-value0.05). However, when segment width was adjusted to 425ms, MCA

increased by 0.87 percent, 1.58 percent, and 2.6 percent for all datasets, respectively (P value=0.98). Similarly, extending the segment width from 50 to 275 milliseconds raised the MCA values of datasets 1, 2, and 3 by 19.37 percent, 13.66 percent, and 18.98 percent, respectively (P-value0.05). Alternatively, increasing the segment length from 275 to 450ms raised MCA by 0.84, 1.31, and 1.76 percent, respectively (P-value=0.12).

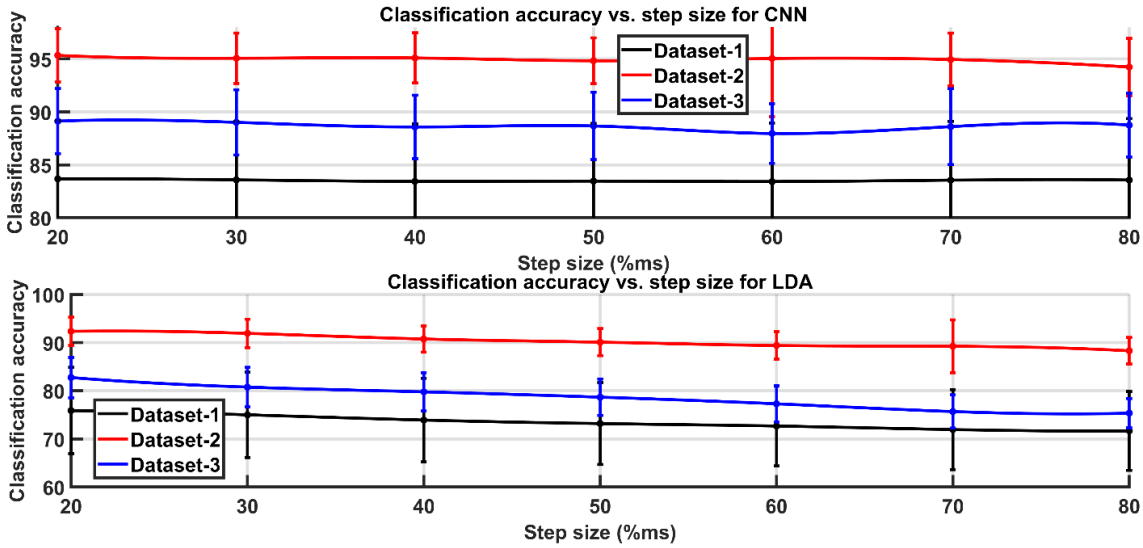

Figure 12. Classification accuracy corresponding to CNN and LDA with respect to different overlap sizes for all the datasets.

4.4 iEMG Segmentation

To determine the optimal window widths for disjoint and overlap windowing, 19 alternative window sizes ranging in length from 50ms to 500ms were selected for both methods. It is important to note that, since overlap windowing is defined by the window and the step/overlap width, the MCA value of all overlap sizes is used to acquire MCA (MMCA) average for each given window size. The connection between CA and increasing

window size is shown in Figure 5 for both windowing methods on both datasets. CA rises as the window size of 50ms increases to 500ms.

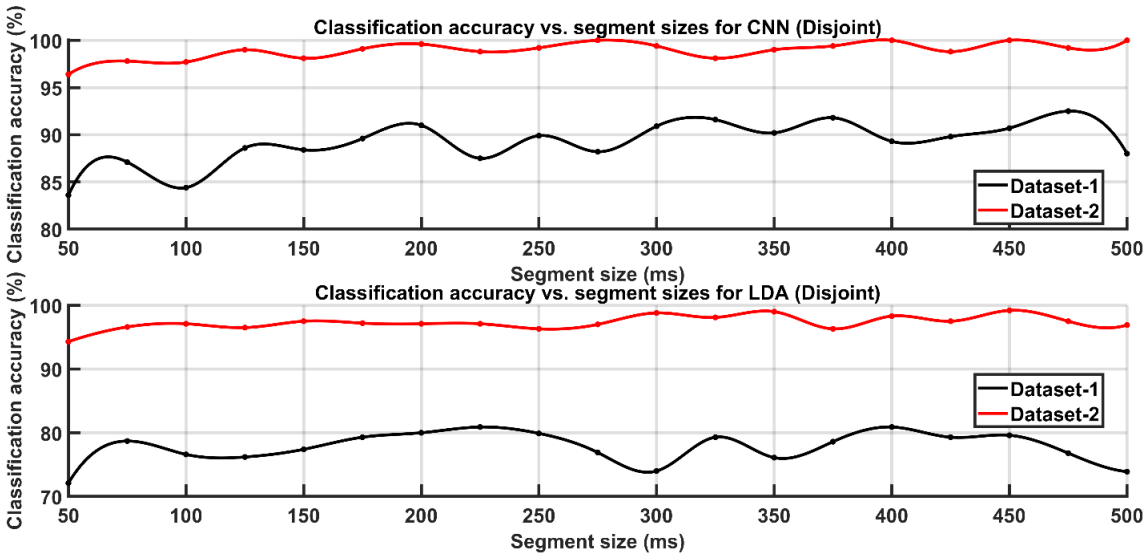

Figure 13. Classification accuracy corresponding to CNN and LDA with respect to different segment sizes for all the datasets of iEMG signals.

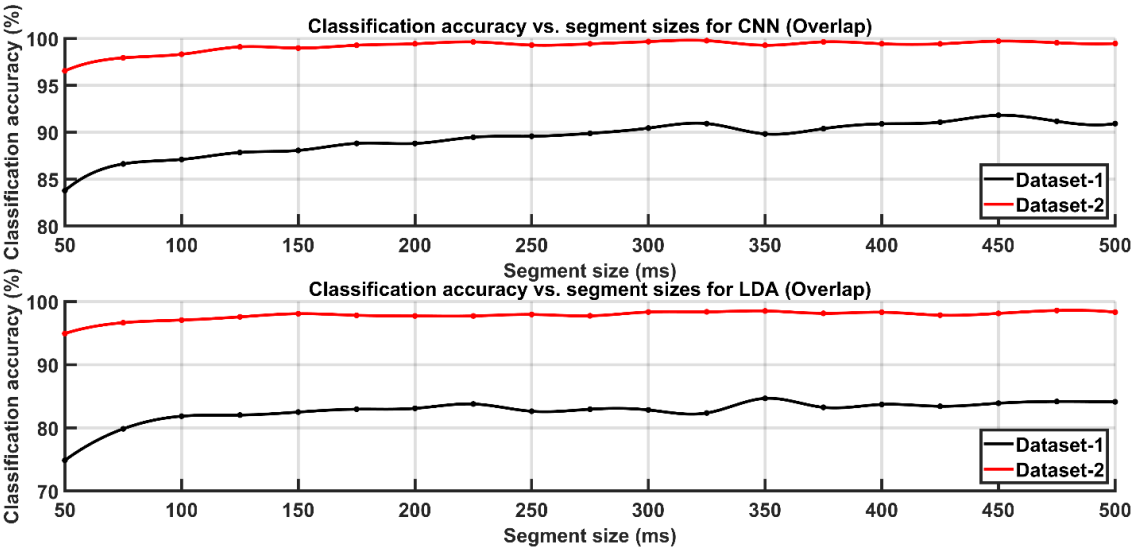

Figure 14. Classification accuracy corresponding to CNN and LDA with respect to different overlap sizes for all the datasets of iEMG signals.

Table 3. MCAs for dataset-1 across varying window and overlap size.

O.S (%) / W.S (ms)	**10**	**20**	**30**	**40**	**50**	**60**	**70**	**80**	**90**
50	83.6	84.1	84.0	83.7	84.8	84.0	83.7	83.1	83.0
75	86.8	86.8	86.7	86.9	85.9	85.5	86.3	88.2	86.7
100	87.6	87.6	87.4	87.1	86.5	86.7	86.8	85.9	88.4
125	88.4	88.5	87.6	88.4	87.4	87.6	87.7	87.5	87.7
150	88.6	89.2	88.1	88.5	88.1	87.2	88.1	88.5	86.4
175	89.2	89.3	89.1	89.4	87.8	89.3	88.6	88.5	88.3
200	89.6	90.0	89.0	87.7	89.2	88.7	88.7	88.7	87.7
225	89.8	89.3	89.6	89.2	89.1	90.7	88.2	89.0	90.5
250	91.5	90.7	89.9	91.1	89.2	88.9	88.0	88.4	88.6
275	90.9	89.9	89.0	91.0	89.1	90.2	90.3	90.3	88.4
300	91.2	90.8	92.1	90.9	89.7	91.6	89.2	89.5	88.9
325	91.3	90.6	90.4	91.1	89.6	92.3	92.0	91.2	89.8
350	91.5	91.6	90.1	90.4	88.7	90.6	89.1	87.4	89.1
375	91.9	90.6	90.5	91.7	90.3	90.5	89.1	89.1	89.8
400	91.8	92.7	92.9	91.6	91.9	87.4	89.5	91.5	88.9
425	91.7	91.2	92.9	92.4	90.3	90.0	91.3	88.9	91.1
450	92.2	92.9	92.0	92.0	91.5	93.3	91.8	89.8	90.9
475	92.1	92.4	92.2	91.8	92.1	90.9	89.1	88.2	91.8
500	93.2	91.8	91.0	90.7	90.7	90.3	89.8	92.7	88.2

Table 4. MCAs for dataset-2 across varying window and overlap size.

O.S (%) / W.S (ms)	**10**	**20**	**30**	**40**	**50**	**60**	**70**	**80**	**90**
50	96.7	96.8	96.3	96.2	96.1	96.6	97.0	96.5	96.8
75	97.8	98.1	98.0	98.4	97.7	97.6	98.2	97.7	98.1
100	98.6	96.7	98.8	98.6	98.4	98.7	97.9	98.3	98.9
125	99.0	99.1	99.1	98.8	99.0	99.4	99.1	99.4	99.2
150	99.1	99.4	99.1	98.9	98.8	99.3	99.4	98.0	98.9
175	99.4	99.5	99.2	99.2	99.5	99.2	99.0	99.2	99.5
200	99.3	99.3	99.4	99.8	99.6	99.3	99.2	99.7	99.4
225	99.7	99.5	99.7	99.6	100.0	98.9	99.7	100.0	99.6
250	99.7	99.6	99.5	99.6	99.6	99.2	99.3	98.9	98.3
275	99.5	99.7	99.2	99.6	99.2	99.6	99.2	99.6	99.5
300	99.6	100.0	99.8	99.6	99.5	100.0	100.0	99.2	99.5
325	99.8	99.5	99.6	99.8	99.7	99.6	100.0	100.0	100.0
350	99.6	99.7	99.6	98.9	100.0	98.3	100.0	98.8	98.8
375	99.5	99.6	99.6	100.0	100.0	99.2	99.5	99.5	100.0
400	99.8	99.7	99.8	99.7	99.6	99.6	98.8	99.4	98.8
425	99.9	99.8	99.8	99.7	98.9	99.0	99.0	100.0	98.8
450	99.8	99.6	99.8	100.0	100.0	99.5	99.4	99.4	100.0
475	99.4	99.6	99.7	100.0	99.6	98.8	99.5	99.4	100.0
500	99.8	99.6	99.7	99.6	100.0	99.0	100.0	98.1	99.4

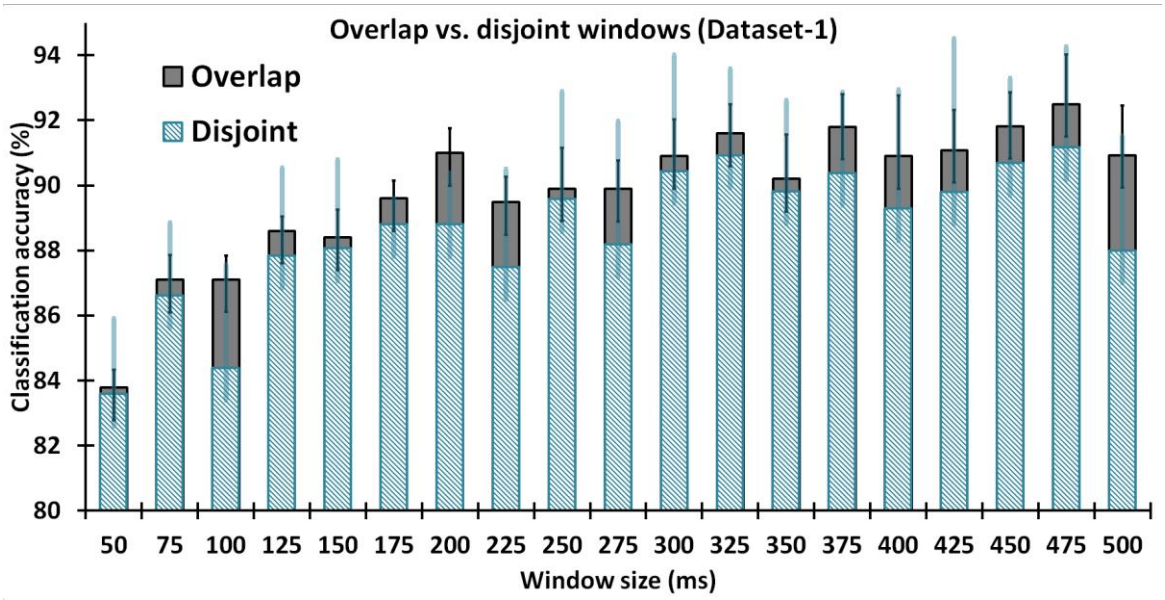

Figure 15. Classification accuracy for dataset-1 of iEMG signals.

In case of datasets 1, the greatest and lowest accuracies were obtained with window sizes of 475ms and 50ms, respectively, with MCAs of 92.5 percent 6.16 and 83.62 percent 4.6. As shown in Figure 5, the MCA rises substantially from 83.62 percent 4.6 to 91.033.1 when the window size of 50ms is increased to 200ms. However, variation of window size between 200ms and 500ms causes no substantial improvement in MCA (only step width of 1.47 percent). Similarly, for dataset 2, the maximum and minimum MCA values were 96.35 percent 3.3 and 99.17 percent 1.52, respectively, for 50ms and 275ms window sizes. MCA rises substantially when the extension of window size of 50ms, to 275ms is performed but subsequently does not change much in dataset 2.

With window widths of 50ms and 450ms, the lowest and maximum of CAs are discovered for dataset 1, with MMCAs of 83.77 percent 0.55 and 91.82 percent 1.04. Figure 5 shows that altering the window widths between 50ms and 275ms has a significant impact on MMCA; however, beyond 275ms, there is no significant effect on MMCA. The MMCA with a window size of 450ms, the highest reported MMCA in dataset-1, is significantly different from MMCAs with window widths ranging from 50ms to 275ms, according to ANOVA (P-values 0.05). For window widths of 50ms and 225ms, the lowest and

maximum CAs were 96.550.32 and 99.640.33, respectively, for dataset 2. Furthermore, when the aperture size is increased from 50-225ms, the CA for dataset-2 improves significantly; however, no further improvement in accuracy is observed when the segment length increases.

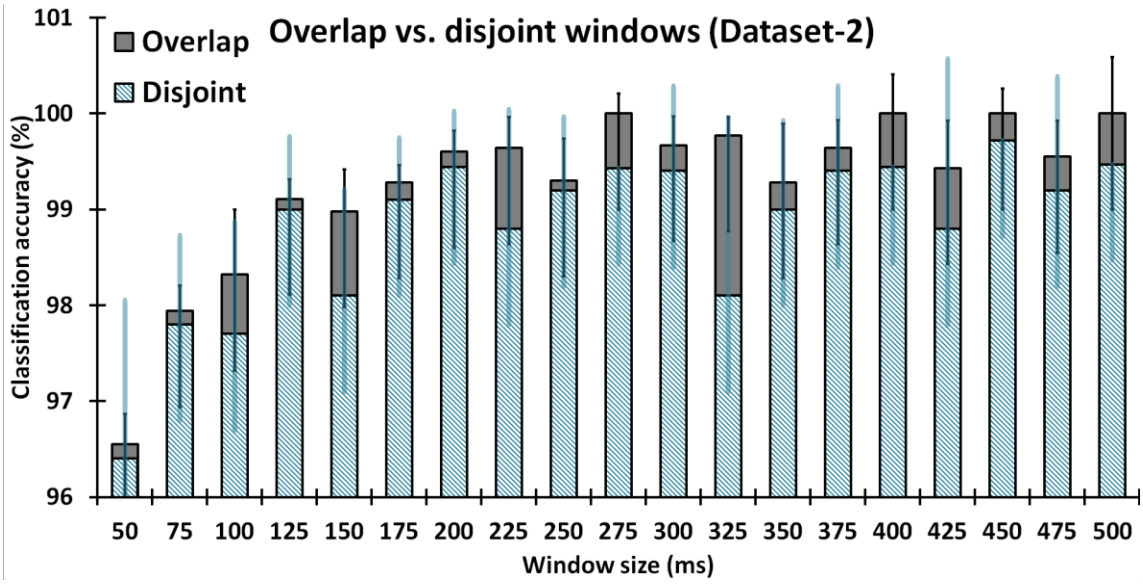

Figure 16. Classification accuracy for dataset-2 of iEMG signals.

Chapter 5

5 Discussion and Conclusion

The aim of this research was to determine and investigate the effectiveness of EMD in denoising EMG data with varying degrees of noise. Additionally, the performance of different thresholding methods and thresholding operators for EMD-based denoising of EMG signals is examined. The findings shown that utilizing EMD-based denoising methods, EMG signals may be filtered out and the impact of noise reduced. This research examines the performance of IT, IIT, and CIIT thresholding methods, as well as the SOFT, HARD, and SCAD thresholding operators. The IIT thresholding technique combined with the HARD thresholding operator produces the best denoising results for EMG signals in terms of SNR, but it fails to preserve the shape of the original signal and results in discontinuities in the denoised EMG signal, regardless of the level of noise contamination. While IIT with SOFT thresholding operator produces somewhat lower SNR values when denoising EMG signals, it effectively maintains the smoothness and features of the original signal. The inferred findings may be used to remove different kinds of noise from EMG signals while retaining the original signal's properties.

Similarly, VMD-based different EMG filters were explored to denoise sEMG and iEMG signals by incorporating different thresholding techniques and operators. It has been found that VMD based EMG filters outperform EMD based EMG filters with respect to SNR values. The best results have been resulted from IIT thresholding technique and SOFT thresholding operator.

The goal of this study was to find out more about if any optimal segment size limitations are found for the sEMG signals segmentation without any connection to the sample frequency used for data collection. To do this, the training and evaluation of all three datasets has been performed on a variety of segment sizes using both methods of segmentation and both classifiers. CA has been found to grow consistently as segment size increases. CA increases proportionately as segment size increases from 50ms to 250ms for each classifier and found no differences in classification accuracies when segment size is increased from 250-450ms for either LDA or CNN. Increases in segment length above

325ms have little impact on categorization output; on the contrary, they increase computation load to the point where it exceeds the real-time MEC delay time limit. Change the fragment size for discontinuous differentiation to between 250-300ms without affecting the delay duration to obtain the best classification accuracies for steady MEC. There was no significant variation in classification accuracies between segment sizes 250-450ms for LDA with crossover division. In the case of CNN with interchange separation, there was no huge discrepancy in MCA between slice sizes of 275-450ms. Because real-time MEC is limited to component sizes of less than 300ms, the best CA may be obtained by employing overlay delineation with fragment sizes well below 1ms.

The goal of this research was to find the best compositing strategy for an iEMG-based monitoring, diagnosis, and recognition method The data was pre-processed to remove extraneous noise from the collected signals in order to do this. As seen in Figure 4, the filters used significantly improve classification accuracy while also reducing noise in the data. On two separately documented databases of iEMG signals, we examined both discontinuous and wraparound compositing methods, as well as different window widths. The impact of changing the overlap frame in the overlap compositing technique on the system's optimum performance has also been studied and measured. For reflectance spectra of EMG data and the development of a system classification accuracy suitable of categorising EMG signals, the length of the session should also be compatible with the time delay restriction in real-time function. The offline equitable distribution may be integrated into a device that can do real-time activities with high classification accuracy. Only when the window width is extended for both datasets does the classification accuracy improve. Statistics showed that expanding the window size from 50-200ms improves classification accuracy utilises it to oscillate up and down till 500ms on both datasets. On combined datasets, the classification accuracy increased from 89.27 to 94.83 percent when the window size was changed from 50-200ms. Following that, there was no discernible difference in categorization accuracy.

Similarly, when the window duration is altered from 50-225ms for both iEMG recordings and statistically analysed, it was found that MMCA substantially rises from 90.16 to 94.56 percent. No statistically significant change was found in MMCA with window sizes greater

than 225ms (P-values > 0.05). The findings indicate that the optimal window durations for disjoint and overlap window methods are 200–300ms and 225–300ms, respectively, recognizing the real-time constraint of segment length in relation to the optimal window size for an intramuscular EMG diagnostic, detection, and myoelectric system. The derived findings have been found consistent with the operating rules of actual myoelectric system. According to [54], the window size for a real-time control system utilized in an assistive and assisstive robotic device ought to be smaller than 300ms. Nonetheless, the optimal window widths found for both disjoint and overlap methods vary from those discovered for sEMG-based control systems. According to [21], the optimal window widths for overlap and disjoint window methods are 250ms and 300ms for an analytical system based on sEMG.

5.1 Conclusion

The study's primary objective was to develop an optimum myoelectric control technique. To accomplish this, several EMG denoising methods were explored to remove noise from the EMG data. Two signal decomposition methods were utilized to breakdown the EMG signals: EMD and VMD. Denoising of the decomposed EMG signals was accomplished via the use of IT, IIT, and CIIT thresholding methods in conjunction with SOFT, HARD, and SCAD thresholding operators. The findings indicate that VMD-based EMG filters beat EMD-based EMG filters in terms of SNR for both sEMG and iEMG signals. Similarly, IIT thresholding methods outperform conventional thresholding techniques by maintaining the intrinsic features of the EMG signals. Additionally, it was discovered that the SOFT thresholding operator beats other thresholding operators in terms of resultant SNR values.

Additionally, the research examined different segmentation or windowing methods to determine the optimal segment and overlap size for EMG data and it has been discovered that when compared to disjoint segmentation or windowing, overlap segmentation or windowing produces the highest classification performance outcomes. Additionally, the findings indicated that the performance of the MEC system improves with increasing segment size. However, when the overlap size is reduced, the performance degrades.

6 References

[1]. Merletti, R. and Di Torino, P.J.J.E.K., 1999. Standards for reporting EMG data. J Electromyogr Kinesiol, 9(1), pp.3-4.

[2]. Hubbard, D.R. and Berkoff, G.M., 1993. Myofascial trigger points show spontaneous needle EMG activity. Spine, 18(13), pp.1803-1807.

[3]. Bunzynski, T.H., Stoyva, J.M., Adler, C.S. and Mullaney, D.J., 1973. EMG biofeedback and tension headache: a controlled outcome study. Psychosomatic medicine.

[4]. Woods, J.J. and Bigland-Ritchie, B., 1983. Linear and non-linear surface EMG/force relationships in human muscles. An anatomical/functional argument for the existence of both. American journal of physical medicine, 62(6), pp.287-299.

[5]. Dobkin, B.H., Harkema, S., Requejo, P. and Edgerton, V.R., 1995. Modulation of locomotor-like EMG activity in subjects with complete and incomplete spinal cord injury. Journal of neurologic rehabilitation, 9(4), pp.183-190.

[6]. Mirka, G.A., 1991. The quantification of EMG normalization error. Ergonomics, 34(3), pp.343-352.

[7]. Bigland-Ritchie, B., Johansson, R., Lippold, O.C. and Woods, J.J., 1983. Contractile speed and EMG changes during fatigue of sustained maximal voluntary contractions. Journal of neurophysiology, 50(1), pp.313-324.

[8]. Winter, D.A. and Yack, H.J., 1987. EMG profiles during normal human walking: stride-to-stride and inter-subject variability. Electroencephalography and clinical neurophysiology, 67(5), pp.402-411.

[9]. Bigland-Ritchie, B., Donovan, E.F. and Roussos, C.S., 1981. Conduction velocity and EMG power spectrum changes in fatigue of sustained maximal efforts. Journal of applied physiology, 51(5), pp.1300-1305.

[10]. Alkner, B.A., Tesch, P.A. and Berg, H.E., 2000. Quadriceps EMG/force relationship in knee extension and leg press. Medicine and science in sports and exercise, 32(2), pp.459-463.

[11]. Jobe, F.W., Moynes, D.R., Tibone, J.E. and Perry, J., 1984. An EMG analysis of the shoulder in pitching: a second report. The American journal of sports medicine, 12(3), pp.218-220.

[12]. Yao, W., Fuglevand, R.J. and Enoka, R.M., 2000. Motor-unit synchronization increases EMG amplitude and decreases force steadiness of simulated contractions. Journal of neurophysiology, 83(1), pp.441-452.

[13]. Holroyd, K.A., Penzien, D.B., Hursey, K.G., Tobin, D.L., Rogers, L., Holm, J.E., Marcille, P.J., Hall, J.R. and Chila, A.G., 1984. Change mechanisms in EMG biofeedback training: cognitive changes underlying improvements in tension headache. Journal of consulting and clinical psychology, 52(6), p.1039.

[14]. Marsh, A.P. and Martin, P.E., 1995. The relationship between cadence and lower extremity EMG in cyclists and noncyclists. Medicine and science in sports and exercise, 27(2), pp.217-225.

[15]. Komi, P.V. and Tesch, P., 1979. EMG frequency spectrum, muscle structure, and fatigue during dynamic contractions in man. European journal of applied physiology and occupational physiology, 42(1), pp.41-50.

[16]. Isear Jr, J.A., Erickson, J.C. and Worrell, T.W., 1997. EMG analysis of lower extremity muscle recruitment patterns during an unloaded squat. Medicine and science in sports and exercise, 29(4), pp.532-539.
[17]. Moseley JR, J.B., Jobe, F.W., Pink, M., Perry, J. and Tibone, J., 1992. EMG analysis of the scapular muscles during a shoulder rehabilitation program. The American journal of sports medicine, 20(2), pp.128-134.
[18]. Perry, J. and Bekey, G.A., 1981. EMG-force relationships in skeletal muscle. Critical reviews in biomedical engineering, 7(1), pp.1-22.
[19]. Farina, D. and Merletti, R., 2000. Comparison of algorithms for estimation of EMG variables during voluntary isometric contractions. Journal of Electromyography and Kinesiology, 10(5), pp.337-349.
[20]. Graupe, D. and Cline, W.K., 1975. Functional separation of EMG signals via ARMA identification methods for prosthesis control purposes. IEEE Transactions on Systems, Man, and Cybernetics, (2), pp.252-259.
[21]. Cholewicki, J., McGill, S.M. and Norman, R.W., 1995. Comparison of muscle forces and joint load from an optimization and EMG assisted lumbar spine model: towards development of a hybrid approach. Journal of biomechanics, 28(3), pp.321-331.
[22]. Ahern, D.K., Follick, M.J., Council, J.R., Laser-Wolston, N. and Litchman, H., 1988. Comparison of lumbar paravertebral EMG patterns in chronic low back pain patients and non-patient controls. Pain, 34(2), pp.153-160.
[23]. Manns, A., Miralles, R. and Palazzi, C., 1979. EMG, bite force, and elongation of the masseter muscle under isometric voluntary contractions and variations of vertical dimension. The Journal of prosthetic dentistry, 42(6), pp.674-682.
[24]. Thorstensson, A., Karlsson, J., Viitasalo, J.H.T., Luhtanen, P. and Komi, P.V., 1976. Effect of strength training on EMG of human skeletal muscle. Acta Physiologica Scandinavica, 98(2), pp.232-236.
[25]. Lundberg, U., Kadefors, R., Melin, B., Palmerud, G., Hassmén, P., Engström, M. and Dohns, I.E., 1994. Psychophysiological stress and EMG activity of the trapezius muscle. International journal of behavioral medicine, 1(4), pp.354-370.
[26]. Mathiassen, S.E., Winkel, J. and Hägg, G.M., 1995. Normalization of surface EMG amplitude from the upper trapezius muscle in ergonomic studies—a review. Journal of electromyography and kinesiology, 5(4), pp.197-226.
[27]. Hiraiwa, A., Shimohara, K. and Tokunaga, Y., 1989, November. EMG pattern analysis and classification by neural network. In Conference Proceedings., IEEE International Conference on Systems, Man and Cybernetics (pp. 1113-1115). IEEE.
[28]. Day, B.L., Dressler, D., Maertens de Noordhout, A.C.D.M., Marsden, C.D., Nakashima, K., Rothwell, J.C. and Thompson, P.D., 1989. Electric and magnetic stimulation of human motor cortex: surface EMG and single motor unit responses. The Journal of physiology, 412(1), pp.449-473.
[29]. Hallett, M.A.R.K., Shahani, B.T. and Young, R.R., 1975. EMG analysis of stereotyped voluntary movements in man. Journal of Neurology, Neurosurgery & Psychiatry, 38(12), pp.1154-1162.
[30]. Viitasalo, J.H. and Komi, P.V., 1977. Signal characteristics of EMG during fatigue. European journal of applied physiology and occupational physiology, 37(2), pp.111-121.

[31]. Arendt-Nielsen, L. and Mills, K.R., 1985. The relationship between mean power frequency of the EMG spectrum and muscle fibre conduction velocity. Electroencephalography and clinical Neurophysiology, 60(2), pp.130-134.
[32]. Zardoshti-Kermani, M., Wheeler, B.C., Badie, K. and Hashemi, R.M., 1995. EMG feature evaluation for movement control of upper extremity prostheses. IEEE Transactions on Rehabilitation Engineering, 3(4), pp.324-333.
[33]. Roy, R.R., Hutchison, D.L., Pierotti, D.J., Hodgson, J.A. and Edgerton, V.R., 1991. EMG patterns of rat ankle extensors and flexors during treadmill locomotion and swimming. Journal of applied physiology, 70(6), pp.2522-2529.
[34]. Burden, A. and Bartlett, R., 1999. Normalisation of EMG amplitude: an evaluation and comparison of old and new methods. Medical engineering & physics, 21(4), pp.247-257.
[35]. Redfern, M.S., Hughes, R.E. and Chaffin, D.B., 1993. High-pass filtering to remove electrocardiographic interference from torso EMG recordings. Clinical Biomechanics, 8(1), pp.44-48.
[36]. Berardelli, A., Dick, J.P., Rothwell, J.C., Day, B.L. and Marsden, C.D., 1986. Scaling of the size of the first agonist EMG burst during rapid wrist movements in patients with Parkinson's disease. Journal of Neurology, Neurosurgery & Psychiatry, 49(11), pp.1273-1279.
[37]. Ferraccioli, G., Ghirelli, L., Scita, F., Nolli, M., Mozzani, M., Fontana, S., Scorsonelli, M., Tridenti, A. and De Risio, C., 1987. EMG-biofeedback training in fibromyalgia syndrome. The Journal of Rheumatology, 14(4), pp.820-825.
[38]. Petrofsky, J.S. and Lind, A.R., 1980. The influence of temperature on the amplitude and frequency components of the EMG during brief and sustained isometric contractions. European Journal of Applied Physiology and Occupational Physiology, 44(2), pp.189-200.
[39]. Mambrito, B. and De Luca, C.J., 1984. A technique for the detection, decomposition and analysis of the EMG signal. Electroencephalography and clinical neurophysiology, 58(2), pp.175-188.
[40]. Tesch, P.A., Dudley, G.A., Duvoisin, M.R., Hather, B.M. and Harris, R.T., 1990. Force and EMG signal patterns during repeated bouts of concentric or eccentric muscle actions. Acta Physiologica Scandinavica, 138(3), pp.263-271.
[41]. Hakkinen, K., Kallinen, M., Izquierdo, M., Jokelainen, K., Lassila, H., Malkia, E., Kraemer, W.J., Newton, R.U. and Alen, M., 1998. Changes in agonist-antagonist EMG, muscle CSA, and force during strength training in middle-aged and older people. Journal of applied physiology, 84(4), pp.1341-1349.
[42]. Chan, F.H., Yang, Y.S., Lam, F.K., Zhang, Y.T. and Parker, P.A., 2000. Fuzzy EMG classification for prosthesis control. IEEE transactions on rehabilitation engineering, 8(3), pp.305-311.
[43]. Reimers-Neils, L., Logemann, J. and Larson, C., 1994. Viscosity effects on EMG activity in normal swallow. Dysphagia, 9(2), pp.101-106.
[44]. Bø, K. and Stien, R., 1994. Needle EMG registration of striated urethral wall and pelvic floor muscle activity patterns during cough, Valsalva, abdominal, hip adductor, and gluteal muscle contractions in nulliparous healthy females. Neurourology and urodynamics, 13(1), pp.35-41.

[45]. Vrana, S.R., 1993. The psychophysiology of disgust: Differentiating negative emotional contexts with facial EMG. Psychophysiology, 30(3), pp.279-286.
[46]. Crider, A.B. and Glaros, A.G., 1999. A meta-analysis of EMG biofeedback treatment of temporomandibular disorders. Journal of Orofacial Pain, 13(1).
[47]. Cholewicki, J. and McGill, S.M., 1994. EMG assisted optimization: a hybrid approach for estimating muscle forces in an indeterminate biomechanical model. Journal of biomechanics, 27(10), pp.1287-1289.
[48]. Calancie, B., Madsen, P. and Lebwohl, N., 1994. Stimulus-evoked EMG monitoring during transpedicular lumbosacral spine instrumentation. Initial clinical results. Spine, 19(24), pp.2780-2786.
[49]. Ng, J.K., Kippers, V. and Richardson, C.A., 1998. Muscle fibre orientation of abdominal muscles and suggested surface EMG electrode positions. Electromyography and clinical neurophysiology, 38(1), pp.51-58.
[50]. Masuda, K., Masuda, T., Sadoyama, T., Inaki, M. and Katsuta, S., 1999. Changes in surface EMG parameters during static and dynamic fatiguing contractions. Journal of electromyography and kinesiology, 9(1), pp.39-46.
[51]. Park, S.H. and Lee, S.P., 1998. EMG pattern recognition based on artificial intelligence techniques. IEEE transactions on Rehabilitation Engineering, 6(4), pp.400-405.
[52]. Nummela, A., Rusko, H.E.I.K.K.I. and Mero, A.N.T.T.I., 1994. EMG activities and ground reaction forces during fatigued and nonfatigued sprinting. Medicine and science in sports and exercise, 26(5), pp.605-609.
[53]. Murray, M.P., Mollinger, L.A., Gardner, G.M. and Sepic, S.B., 1984. Kinematic and EMG patterns during slow, free, and fast walking. Journal of Orthopaedic Research, 2(3), pp.272-280.
[54]. Hogan, N., 1976. A review of the methods of processing EMG for use as a proportional control signal. Biomedical engineering, 11(3), pp.81-86.
[55]. Akazawa, K., Milner, T.E. and Stein, R.B., 1983. Modulation of reflex EMG and stiffness in response to stretch of human finger muscle. Journal of neurophysiology, 49(1), pp.16-27.
[56]. Solomonow, M., Baratta, R., Bernardi, M., Zhou, B., Lu, Y., Zhu, M. and Acierno, S., 1994. Surface and wire EMG crosstalk in neighbouring muscles. Journal of Electromyography and Kinesiology, 4(3), pp.131-142.
[57]. Turton, A., Wroe, S., Trepte, N., Fraser, C. and Lemon, R.N., 1996. Contralateral and ipsilateral EMG responses to transcranial magnetic stimulation during recovery of arm and hand function after stroke. Electroencephalography and Clinical Neurophysiology/Electromyography and Motor Control, 101(4), pp.316-328.
[58]. Petrofsky, J.S., Glaser, R.M., Phillips, C.A., Lind, A.R. and Williams, C., 1982. Evaluation of the amplitude and frequency components of the surface EMG as an index of muscle fatigue. Ergonomics, 25(3), pp.213-223.
[59]. Jorge, M. and Hull, M.L., 1986. Analysis of EMG measurements during bicycle pedalling. Journal of biomechanics, 19(9), pp.683-694.
[60]. Tangel, D.J., Mezzanotte, W.S. and White, D.P., 1991. Influence of sleep on tensor palatini EMG and upper airway resistance in normal men. Journal of applied physiology, 70(6), pp.2574-2581.

[61]. Yang, J.F. and Winter, D.A., 1985. Surface EMG profiles during different walking cadences in humans. Electroencephalography and clinical Neurophysiology, 60(6), pp.485-491.
[62]. Hazlett, R.L. and Hazlett, S.Y., 1999. Emotional response to television commercials: Facial EMG vs. self-report. Journal of advertising research, 39(2), pp.7-7.
[63]. Komi, P.V., Linnamo, V.E.S.A., Silventoinen, P.E.R.T.T.I. and Sillanpaa, M., 2000. Force and EMG power spectrum during eccentric and concentric actions. Medicine and Science in sports and Exercise, 32(10), pp.1757-1762.
[64]. Granata, K.P. and Marras, W.S., 1995. An EMG-assisted model of trunk loading during free-dynamic lifting. Journal of biomechanics, 28(11), pp.1309-1317.
[65]. Visser, C.P.J., Coene, L.N.J.E.M., Brand, R. and Tavy, D.L.J., 1999. The incidence of nerve injury in anterior dislocation of the shoulder and its influence on functional recovery: a prospective clinical and EMG study. The Journal of bone and joint surgery. British volume, 81(4), pp.679-685.
[66]. Arendt-Nielsen, L., Mills, K.R. and Forster, A., 1989. Changes in muscle fiber conduction velocity, mean power frequency, and mean EMG voltage during prolonged submaximal contractions. Muscle & Nerve: Official Journal of the American Association of Electrodiagnostic Medicine, 12(6), pp.493-497.
[67]. Bigland-Ritchie, B., 1981. EMG/force relations and fatigue of human voluntary contractions. Exercise and sport sciences reviews, 9(1), pp.75-118.
[68]. Bigland-Ritchie, B., 1981. EMG/force relations and fatigue of human voluntary contractions. Exercise and sport sciences reviews, 9(1), pp.75-118.
[69]. Harris, D.V. and Robinson, W.J., 1986. The effects of skill level on EMG activity during internal and external imagery. Journal of Sport and Exercise Psychology, 8(2), pp.105-111.
[70]. Potvin, J.R. and Bent, L.R., 1997. A validation of techniques using surface EMG signals from dynamic contractions to quantify muscle fatigue during repetitive tasks. Journal of Electromyography and Kinesiology, 7(2), pp.131-139.
[71]. Stålberg, E. and Fawcett, P.R., 1982. Macro EMG in healthy subjects of different ages. Journal of Neurology, Neurosurgery & Psychiatry, 45(10), pp.870-878.
[72]. Hagg, G.M., 1992. Interpretation of EMG spectral alterations and alteration indexes at sustained contraction. Journal of Applied Physiology, 73(4), pp.1211-1217.
[73]. David, G.A.J.M., Magarey, M.E., Jones, M.A., Dvir, Z., Türker, K.S. and Sharpe, M., 2000. EMG and strength correlates of selected shoulder muscles during rotations of the glenohumeral joint. Clinical biomechanics, 15(2), pp.95-102.
[74]. David, G.A.J.M., Magarey, M.E., Jones, M.A., Dvir, Z., Türker, K.S. and Sharpe, M., 2000. EMG and strength correlates of selected shoulder muscles during rotations of the glenohumeral joint. Clinical biomechanics, 15(2), pp.95-102.
[75]. Granata, K.P. and Marras, W.S., 1993. An EMG-assisted model of loads on the lumbar spine during asymmetric trunk extensions. Journal of biomechanics, 26(12), pp.1429-1438.
[76]. Calancie, B., Lebwohl, N., Madsen, P. and Klose, K.J., 1992. Intraoperative evoked EMG monitoring in an animal model. A new technique for evaluating pedicle screw placement. Spine, 17(10), pp.1229-1235.
[77]. Werhahn, K.J., Fong, J.K.Y., Meyer, B.U., Priori, A., Rothwell, J.C., Day, B.L. and Thompson, P.D., 1994. The effect of magnetic coil orientation on the latency of surface

EMG and single motor unit responses in the first dorsal interosseous muscle. Electroencephalography and Clinical Neurophysiology/Evoked Potentials Section, 93(2), pp.138-146.

Hassan Final

ORIGINALITY REPORT

7%	4%	4%	2%
SIMILARITY INDEX	INTERNET SOURCES	PUBLICATIONS	STUDENT PAPERS

PRIMARY SOURCES

1	Submitted to Higher Education Commission Pakistan Student Paper	2%
2	Mohammed Z., Abbas H.. "Chapter 16 Artificial Human Arm Driven by EMG Signal", IntechOpen, 2012 Publication	1%
3	research.library.mun.ca Internet Source	1%
4	Hassan Ashraf, Asim Waris, Syed Omer Gilani, Amer Sohail Kashif, Mohsin Jamil, Mads Jochumsen, Imran Khan Niazi. "Evaluation of windowing techniques for intramuscular EMG-based diagnostic, rehabilitative and assistive devices", Journal of Neural Engineering, 2020 Publication	<1%
5	vuir.vu.edu.au Internet Source	<1%
6	collections.plymouth.ac.uk Internet Source	<1%